UPPSALA
UNIVERSITET

Digital Comprehensive Summaries of Uppsala Dissertations from the Faculty of Science and Technology 1679

Influence of Aromaticity on Excited State Structure, Reactivity and Properties

KJELL JORNER

ACTA
UNIVERSITATIS
UPSALIENSIS
UPPSALA
2018

ISSN 1651-6214
ISBN 978-91-513-0354-3
urn:nbn:se:uu:diva-349229

Dissertation presented at Uppsala University to be publicly examined in room 80101, Ångströmlaboratoriet, Lägerhyddsvägen 1, Uppsala, Thursday, 14 June 2018 at 13:15 for the degree of Doctor of Philosophy. The examination will be conducted in English. Faculty examiner: Prof. Dr. Rainer Herges (Christian-Albrechts-Universität zu Kiel, Otto-Diels-Institut für Organische Chemie).

Abstract
Jorner, K. 2018. Influence of Aromaticity on Excited State Structure, Reactivity and Properties. *Digital Comprehensive Summaries of Uppsala Dissertations from the Faculty of Science and Technology* 1679. 55 pp. Uppsala: Acta Universitatis Upsaliensis. ISBN 978-91-513-0354-3.

This thesis describes work that could help development of new photochemical reactions and light-absorbing materials. Focus is on the chemical concept "aromaticity" which is a proven conceptual tool in developing thermal chemical reactions. It is here shown that aromaticity is also valuable for photochemistry. The influence of aromaticity is discussed in terms of structure, reactivity and properties. With regard to structure, it is found that photoexcited molecules change their structure to attain aromatic stabilization (planarize, allow through-space conjugation) or avoid antiaromatic destabilization (pucker). As for reactivity, it is found that stabilization/destabilization of reactants decrease/increase photoreactivity, in accordance with the Bell-Evans-Polanyi relationship. Two photoreactions based on excited state antiaromatic destabilization of the substrates are reported. Finally, with respect to properties, it is shown that excited state energies can be tuned by considering aromatic effects of both the electronic ground state and the electronically excited states. The fundamental research presented in this thesis forms a foundation for the development of new photochemical reactions and design of compounds for new organic electronic materials.

Keywords: photochemistry, aromaticity, computational chemistry

Kjell Jorner, Department of Chemistry - Ångström, Box 523, Uppsala University, SE-75120 Uppsala, Sweden.

ISSN 1651-6214
ISBN 978-91-513-0354-3
urn:nbn:se:uu:diva-349229 (http://urn.kb.se/resolve?urn=urn:nbn:se:uu:diva-349229)

List of Papers

This thesis is based on the following papers, which are referred to in the text by their Roman numerals.

I Oh, J., Sung, Y. M., Mori, H., Park, S., Jorner, K., Ottosson, H., Lim, M., Osuka, A., Kim, D. (2017) Unraveling Excited-Singlet-State Aromaticity via Vibrational Analysis. *Chem*, 3:870–880

II Jorner, K., Jahn, B. O., Bultinck, P., Ottosson, H. (2018) Triplet State Homoaromaticity: Concept, Computational Validation and Experimental Relevance. *Chem. Sci.* 9:3165–3176.

III Ueda, M., Jorner, K., Sung, Y. M., Mori, T., Xiao, Q., Kim, D., Ottosson, H., Aida, T., Itoh, Y. (2017) Energetics of Baird Aromaticity Supported by Inversion of Photoexcited Chiral [4*n*]Annulene Derivatives. *Nat. Commun.*, 8:346.

IV Ayub, R., Papadakis, R., Jorner, K., Zietz, B., Ottosson, H. (2017) Cyclopropyl Group: An Excited-State Aromaticity Indicator? *Chem. - Eur. J.*, 23:13684–13695

V Ayub, R., Jorner, K., Ottosson, H. (2017) The Silacyclobutene Ring: An Indicator of Triplet State Baird-Aromaticity. *Inorganics*, 5:91

VI Mohamed, R. K., Mondal, S., Jorner, K., Faria Delgado, T., Lobodin, V. V., Ottosson, H., Alabugin, I. V. (2015) The Missing C1-C5 Cycloaromatization Reaction: Triplet State Antiaromaticity Relief and Self-Terminating Photorelease of Formaldehyde for Synthesis of Fulvenes from Enynes. *J. Am. Chem. Soc.*, 137:15441-15450

VII Papadakis, R., Li, H., Bergman, J., Lundstedt, A., Jorner, K., Ayub, R., Haldar, S., Jahn, B. O., Denisova, A., Zietz, B., Lindh, R., Sanyal, B., Grennberg, H., Leifer, K., Ottosson, H. (2016) Metal-Free Photochemical Silylations and Transfer Hydrogenations of Benzenoid Hydrocarbons and Graphene. *Nat. Commun.*, 7:12962

VIII Jorner, K., Emanuelsson, R., Dahlstrand, C., Tong, H., Denisova, A. V., Ottosson, H. (2014) Impact of Ground- and Excited-State Aromaticity on Cyclopentadiene and Silole Excitation Energies and Excited-State Polarities. *Chem. - Eur. J.*, 20:9295–9303

IX Ayub, R., El Bakouri, O., Jorner, K., Solà, M., Ottosson, H. (2017) Can Baird's and Clar's Rules Combined Explain Triplet State Energies of Polycyclic Conjugated Hydrocarbons with Fused $4n\pi$- and $(4n + 2)\pi$-Rings? *J. Org. Chem.*, 82:6327–6340

X Jorner, K., Feixas, F., Ayub, R., Lindh, R., Solà, M., Ottosson, H. (2016) Analysis of a Compound Class with Triplet States Stabilized by Potentially Baird Aromatic [10]Annulenyl Dicationic Rings. *Chem. - Eur. J.*, 22:2793–2800

Publications not included in this thesis:

I Rudebusch, G. E., Zafra, J. L., Jorner, K., Fukuda, K., Marshall, J. L., Arrechea-Marcos, I., Espejo, G. L., Ponce Ortiz, R., Gómez-García, C. J., Zakharov, L. N., Nakano, M., Ottosson, H., Casado, J., Haley, M. M. (2016) Diindeno-Fusion of an Anthracene as a Design Strategy for Stable Organic Biradicals. *Nat. Chem.*, 8: 753–759

II Lundstedt, A., Papadakis, R., Li, H., Han, Y., Jorner, K., Bergman, J., Leifer, K., Grennberg, H., Ottosson, H. (2017) White-Light Photoassisted Covalent Functionalization of Graphene Using 2-Propanol. *Small Methods*, 1:1700214

III Jorner, K., Dreos, A., Emanuelsson, R., El Bakouri, O., Fdez. Galván, I., Börjesson, K., Feixas, F., Lindh, R., Zietz, B., Moth-Poulsen, K., Ottosson, H. (2017) Unraveling Factors Leading to Efficient Norbornadiene-Quadricyclane Molecular Solar-Thermal Energy Storage Systems. *J. Mater. Chem. A*, 5:12369–12378

IV Poon, J., Yan, J., Jorner, K., Ottosson, H., Donau, C., Singh, V. P., Gates, P. J., Engman, L. (2018) Substituent Effects in Chain-Breaking Aryltellurophenol Antioxidants. *Chem. - Eur. J.*, 24:3520–3527

Contribution report

The author wishes to clarify his contributions to the papers and manuscripts in the thesis.

I Supervised the calculations and co-wrote the manuscript.

II Performed all calculations except the multicenter indices. Wrote the manuscript with feedback from the other authors.

III Performed all calculations and co-wrote the manuscript. Contributed to the original research question.

IV Performed singlet excited state calculations, some of the transition state calculations, supervised the other calculations and co-wrote the manuscript.

V Performed all transition state calculations, supervised the other calculations and co-wrote the manuscript.

VI Performed all calculations, contributed to the mechanistic proposals and co-wrote the manuscript.

VII Performed calculations of hydrogenation energies, aromaticity analysis and co-wrote the manuscript.

VIII Performed approximately half of the calculations, chose the computational methods and wrote the manuscript with contributions from R. Emanuelsson and feedback from H. Ottosson.

IX Performed preliminary work, supervised the calculations, and co-wrote the manuscript.

X Conceived the project together with H. Ottosson and performed all calculations except the FLU aromaticity index. Wrote the manuscript with feedback from H. Ottosson.

Contents

Abbreviations

ACID	Anisotropy of the induced current density
ASE	Aromatic stabilization energy
BEP	Bell-Evans-Polanyi
BLA	Bond-length alternation
CASSCF	Complete active space self-consistent field
CC	Coupled cluster
CD	Circular dichroism
COT	Cyclooctatetraene
cPr	Cyclopropyl
DASD	Dihedral angle standard deviation
DFT	Density functional theory
EDG	Electron-donating group
ES(A)A	Excited state (anti)aromaticity
EWG	Electron-withdrawing group
FLU	Aromatic fluctuation index
HOMA	Harmonic oscillator model of aromaticity
HOMO	Highest occupied molecular orbital
IR	Infrared
IRC	Intrinsic reaction coordinate
ISE	Isomerization stabilization energy
LUMO	Lowest unoccupied molecular orbital
MCI	Multicenter index
MPD	Mean-plane deviation
NICS	Nucleus independent chemical shift
NMR	Nuclear magnetic resonance
PES	Potential energy surface
S_1	First singlet excited state
SA	Shannon aromaticity
SCB	Silacyclobutene
T_1	First triplet excited state
TD-DFT	Time-dependent density functional theory
TRIR	Time-resolved infrared
TS	Transition state
UV-Vis	Ultraviolet-visible
WBI	Wiberg bond index

1 Introduction

Photochemistry occurs when a chemical compound absorbs light of sufficiently high energy to break bonds.[1] The photoexcited molecule can then react either with itself or with other nearby molecules and form new chemical compounds. Photochemistry is central to many important processes in nature, including photosynthesis, vision and production of vitamin D when the body is exposed to sunlight. Organic chemists are trying to use photochemistry in chemical synthesis to make molecules more efficiently or synthesize molecules that are not available by conventional methods. Photochemical routes can potentially also save energy and reduce waste as light delivers energy more precisely than heat.

Unfortunately, the outcome of photochemical reactions is today very difficult to predict and therefore development of new synthesis pathways is slow. The situation is radically different from conventional organic synthesis, where sets of rules and conceptual frameworks have been developed over the last century. With these rules, an experienced organic chemist can quickly come up with a reasonable procedure to synthesize a new compound. For organic photochemistry, these types of rules are instead very rare.

The work presented in this thesis investigates one such rule which has great potential for predicting and explaining photochemistry. It is based on the concept of *aromaticity*,[2] which is one of the most known and useful concepts in organic chemistry. The main principle is that molecules which can be described as aromatic – according to a set of criteria – are extra stable and not prone to react. On the other hand, molecules which are *anti*aromatic are instead extra unstable and prone to react. The idea that aromaticity could be used to describe photoexcited molecules, *excited state aromaticity*, originates from theoretical work in the 1970s,[3,4] but it is only in the last few years that the concept has started to be used more broadly by experimental chemists.

Together with my colleagues and collaborators, I have significantly expanded the knowledge of aromaticity in excited states. In this thesis, I summarize my work by looking at the key molecular aspects of *structure*, *reactivity* and *properties*, and how they can be explained by (anti)aromaticity. First, I ask how molecular *structure* changes upon photoexcitation in response to aromaticity and antiaromaticity. Second, how large is the aromatic stabilization and how is stabilization and destabilization translated into *reactivity*? Can the concept be used to develop two new types of photochemical reactions? Third, can aromaticity be used to tune photophysical *properties*?

2 Background and methods

In this part of the thesis, I first introduce the aromaticity concept and how it can be extended to photoexcited molecules. I then describe how photochemistry can be understood and simulated through computational chemistry. Finally, I discuss the special computational methods used to study aromaticity.

2.1 Aromaticity in ground and excited states

Aromaticity is a corner-stone concept in organic chemistry which describes the special stability of cyclically conjugated molecules with a certain number of π-electrons.[2] Conversely, *antiaromaticity* describes a destabilization. *Hückel's rule* can be used to decide if a molecule is aromatic or antiaromatic:

- Annulenes with $4n$ +2 π-electrons are aromatic
- Annulenes with $4n$ π-electrons are antiaromatic

Aromaticity has been used to describe molecules in the electronic ground state since the 19th century and is a valuable concept for analyzing and predicting structure, properties and reactivity. On the other hand, antiaromaticity can explain why some molecules do not exist and why certain intermediates and transition states are disfavored during chemical reactions.

Aromaticity in photoexcited states

The first clue that aromaticity may be important in excited states came from work on pericyclic reactions. The Woodward-Hoffmann rules[5] are reversed for photochemical reactions, and this was explained independently by Dewar and Zimmerman based on aromatic stabilization or antiaromatic destabilization in the excited state.[6] Baird later generalized this analysis and gave a more rigorous derivation for the first triplet excited state (T_1).[3] Excited state aromaticity can be summarized in *Baird's rule*,[7] which applies to the S_1 and T_1 states:

- Annulenes with $4n$ π-electrons are aromatic
- Annulenes with $4n$ + 2 π-electrons are antiaromatic

As can be seen, Baird's rule is the opposite of Hückel's rule. This is the basis for the principle of *reversal of aromaticity*, that molecules switch aromatic/antiaromatic properties upon photoexcitation.[8] This principle is featured extensively in the work presented in this thesis.

Aspects of aromaticity

While the original defining feature of aromaticity was a special stability relative to a non-cyclically conjugated reference, other characteristic features have later been found. These are the different aspects of aromaticity: energy, geometry, magnetism, electron delocalization and reactivity. With regard to *geometry*, aromatic compounds strive to be planar and bond-equalized. With regard to *magnetic properties*, aromatic molecules have unusually high diamagnetic susceptibility and show large shifts in their NMR spectra. These magnetic properties trace their origin to the *delocalized π-electrons* of aromatic molecules that give rise to a ring-current under an induced magnetic field. Aromatic molecules are also *unusually unreactive* compared to conventional unsaturated compounds. Conversely, antiaromatic compounds are bond-length alternating, prefer non-planar conformations, have opposite magnetic properties compared to aromatic compounds, show low electron delocalization and are very reactive.

There has been much discussion if aromaticity can be defined uniquely.[9] Although the aspects correlate well in almost all cases, there are examples of compound classes where they do not.[10] Such observations have led some researchers to define aromaticity exclusively in terms of one of the aspects, *e.g.*, the magnetic.[11] Others have instead stressed that studies on aromaticity must always assess several aspects.[12] This latter approach is used in this thesis.

2.2 Photochemistry and potential energy surfaces

To understand photochemistry, it is instructive to start from concepts relating to conventional thermal reactions. In the reaction coordinate diagram, chemical reactions are described as the transformation of reactants into products over a barrier (Figure 1a). The collective movement of the atoms during the reaction is described by the reaction coordinate (x axis), and the energy (y axis) depends on these atomic positions. The highest point is called the transition state and defines the barrier height. The *potential energy surface* (PES) can be seen as a more detailed version of the reaction coordinate diagram, where reactants and products correspond to minima and transition states to maxima on a continuous surface (Figure 1b). Excited states are drawn as separate PESs (Figure 1c) which lie higher in energy. If two states have the same spin multiplicity, they can cross in *conical intersections*.[13] Relaxation from the excited state to the ground state through a conical intersection is one way that photochemical reactions can occur.

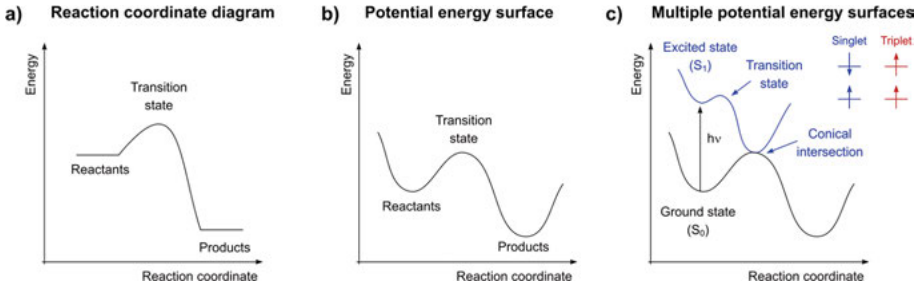

Figure 1. (a) Reaction coordinate diagram. (b) Potential energy surface. (c) Multiple potential energy surfaces in the same diagram.

2.3 Simulating molecular structure, properties and reactivity

The primary method used in this thesis is computational chemistry,[14] which can be used to simulate molecular structure, properties and reactivity. Practically, the minima, transition states and conical intersections are located and characterized, and their relative energies calculated (Figure 1c). The reaction coordinates can be mapped with the *intrinsic reaction coordinate* (IRC) procedure. Molecular properties such as *infrared* (IR) or *ultraviolet-visible* (UV-Vis) absorption spectra are evaluated at the minimum energy (equilibrium) structures.

Computational mapping of PESs is particularly useful for the excited states, where information about structure and reaction pathways is hard to get experimentally. Excited states relevant for organic chemistry have either singlet or triplet *multiplicity* (Figure 1c). Transitions between singlet and triplet states are spin-forbidden and occur through intersystem-crossing and there are no conical intersections between singlet and triplet states. For triplet states, the same computational methods as for the ground state can be used while singlet excited states require more advanced methods.

Computational methods

The workhorse of modern computational chemistry is *density functional theory* (DFT).[15] DFT usually works well for the electronic ground state and has an extension for excited states, *time-dependent DFT* (TD-DFT).[16] However, DFT has problems when the molecule cannot be described by a single electronic configuration, as for organic biradicals and certain electronically excited states.[17] In these cases, the more advanced *Coupled Cluster* (CC) theory[18] or multiconfigurational methods, *e.g.*, the *complete active space self-consistent field* (CASSCF)[19] are needed. The disadvantage is that they take

much longer time and do not always allow for efficient geometry optimizations. For the work in this thesis, I have used mainly DFT and TD-DFT but also CC, CASSCF and related methods when needed.

Although the accuracy of computational methods has increased in the last decades, there are still major challenges, *e.g.*, treatment of solvation and dynamic effects.[20] Another crucial point is that the chosen computational model should correspond to the experimental reality. Reliable predictions from computational chemistry are therefore still rare. These weaknesses can be mitigated by either studying trends across similar molecules or comparing computational and experimental results. I have used both strategies in this thesis.

2.4 Assessing aromaticity

Another key advantage of computational chemistry is that it can study and quantify "fuzzy" chemical concepts[21] such as atomic charge and aromaticity. *Aromaticity indices* are used to assess four of the different aspects of aromaticity: energetic,[22] magnetic[11], geometric[23] and electronic[24]. As the indices do not always agree,[9] it is best to employ several indices of different types.[12] In principle, reactivity could also be used as an index, but this is seldom done.

Energetic indices

Energetic indices estimate the aromatic stabilization or antiaromatic destabilization *vs.* a non-aromatic reference. In this thesis I have employed the *isomerization stabilization energy* method (ISE) which compares the energy of a methylated annulene to its methylene isomer where cyclic conjugation is broken (Figure 2).[25] Aromatic compounds show negative ISE values while antiaromatic compounds show positive values.

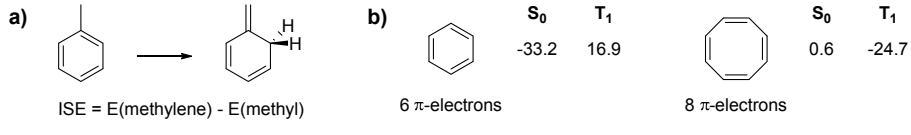

Figure 2. (a) Reaction used to determine ISE with benzene as an example. (b) ISE values in kcal/mol for benzene and cyclooctatetraene (values from ref. 25).

Magnetic indices

Aromatic and antiaromatic compounds have unique magnetic properties due to their induced ring currents. The magnetic indices can be divided into *direct* methods which probe the ring current directly and *indirect* methods which study properties that depend on the ring current.[11]

The *nucleus-independent chemical shift* (NICS) is an indirect method that quantifies the effect of the ring current on NMR chemical shielding constants.[26] One of the best versions is $NICS(1)_{zz}$ which is the negative of the zz-

component of the chemical shielding tensor at 1 Å above the ring plane (Figure 3a).[27] NICS gives a value that can be used to diagnose a compound as aromatic (negative), antiaromatic (positive) or non-aromatic (close to zero). The NICS-Z scan method evaluates NICS on a line perpendicular to the ring plane, going from the ring center to 5 Å above or below the ring. It gives distinct scan profiles that can be used to diagnose aromaticity (Figure 3b).[28] The NICS-XY scan[29] is used for polycyclic systems where the probe atoms are placed on a line across the different rings at a fixed distance of 1.7 Å above the ring plane (Figure 3b).

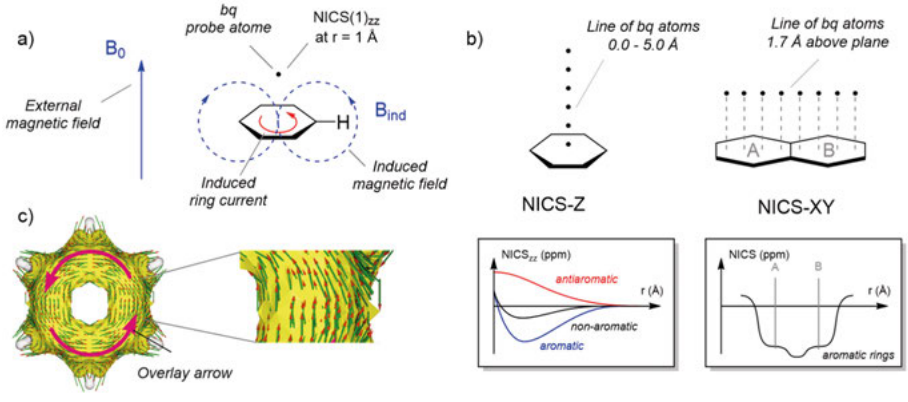

Figure 3. (a) Ring current in benzene under an induced magnetic field with NICS probe atom (called bq). (b) Arrangement of bq atoms to generate a NICS-Z or NICS-XY scan. (c) ACID plot of benzene which is antiaromatic in the T_1 state.

The *anisotropy of the induced current density* (ACID) directly visualizes the direction and magnitude of the ring current (Figure 3c).[30] The length of the arrows indicates the strength of the current. For aromatic molecules the direction of the current is clockwise and for antiaromatic molecule it is counter-clockwise. The general direction of the current is often shown by an overlaid arrow.

Geometric indices

The general trend of lower bond length alternation (BLA) in aromatic compounds and higher BLA in antiaromatic compounds is the basis for the geometric aromaticity indices. The dominating method is the *harmonic oscillator index of aromaticity* (HOMA), where bond length alternation is evaluated against a reference value (R_{opt}).[23]

$$\mathrm{HOMA} = 1 - \frac{\alpha}{n}\sum_{i}^{n}(R_{\mathrm{opt}} - R_i)^2$$

HOMA is normalized with the constant α so that the value for benzene is 1. Positive values indicate aromaticity, negative indicate antiaromaticity and values close to zero indicate non-aromaticity. HOMA can be applied to computer-optimized geometries as well as crystal structure data.

Electronic indices

Aromatic systems feature extensive electron delocalization, which is sampled by electronic indices. The *aromatic fluctuation index* (FLU) measures the uniformity of two-center electron sharing within a ring.[31] Importantly, FLU can be divided into contributions from electrons with α and β spins. In this way it can distinguish between Hückel-aromaticity in which the α and β contributions are equal and Baird-aromaticity where they are not.

Shannon aromaticity (SA) is an electronic index that makes use of the variation of the electron density at the bond centers.[32] Low SA values are obtained for delocalized aromatic systems, while higher values are obtained for antiaromatic and non-aromatic systems for which the bonds differ.

The *multicenter index* (MCI)[33] is an extension of the bond order to an arbitrary number of atoms and can be seen as a direct measure of the extent of electron sharing. Higher values correspond to higher aromaticity while non-aromatic and antiaromatic compounds show low values.

3 Structure

In this chapter I present the main results from two studies that show how excited state aromaticity and antiaromaticity can influence molecular structure in the excited state. In the first study, structural changes due to aromaticity reversal in expanded porphyrins are followed by time-resolved IR spectroscopy in combination with calculations. In the second study, it is shown computationally that photoexcited molecules can change structure to conjugate through space and in this way become aromatic.

3.1 Planarization and distortion (paper I)

The influence of aromaticity on excited state geometries of expanded porphyrins was investigated in collaboration with Prof. Kim and his group (Figure 4a).[34] We studied the ground-state aromatic **1** with 26 π-electrons in the conjugated circuit and the ground-state antiaromatic **2** with 28 π-electrons in the conjugated circuit (Figure 4b). Structural changes were followed experimentally by the Kim group using time-resolved infrared (TRIR) spectroscopy, a technique that can record vibrational spectra on the picosecond time scale. TRIR spectra of **1** and **2** were obtained following photoexcitation to their bright singlet excited states (called S_Q). The selection rules for IR spectroscopy require that a change in dipole moment occurs during the vibration, and excitation of vibrational modes of certain symmetries will be forbidden. TRIR can therefore monitor if the molecule is planarized upon excitation (more symmetric, fewer visible IR bands) or distorted (less symmetric, more visible IR bands).

The experimental results are consistent with excited-state distortion of **1** and planarization of **2**. The simple ground-state IR spectrum of **1** (Figure 5a) is augmented by several new peaks on photoexcitation (Figure 5c). Conversely, the complicated ground-state IR spectrum of **2** (Figure 5b) shows bleach of many peaks on photoexcitation (Figure 5d).

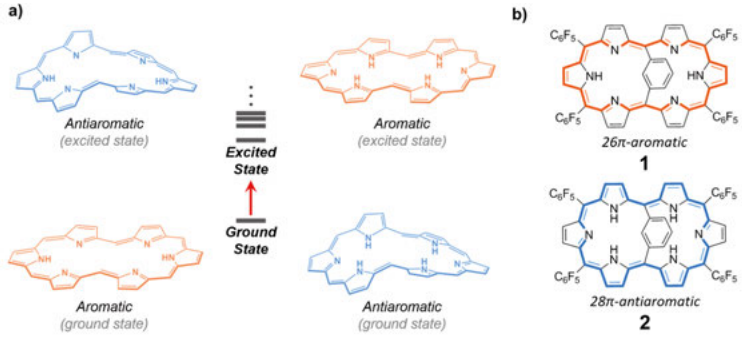

Figure 4. (a) Principle of distortion/symmetrization upon aromaticity reversal. (b) Compounds **1** and **2** studied. Figure reproduced from ref. 34 with permission.

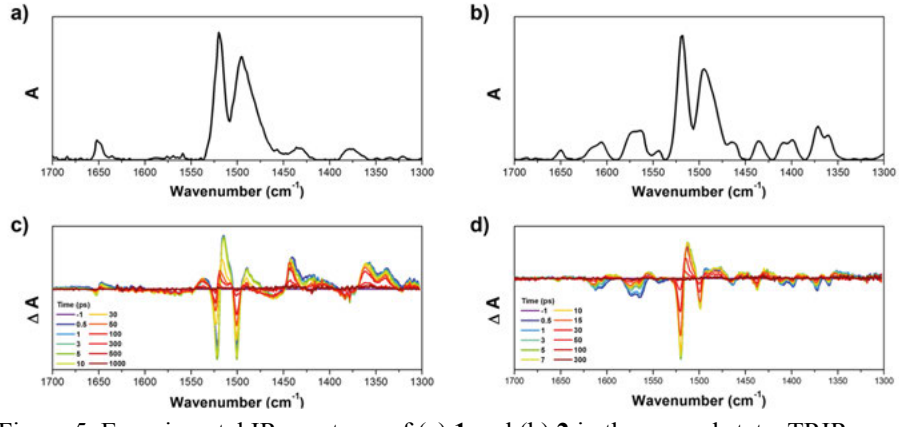

Figure 5. Experimental IR spectrum of (a) **1** and (b) **2** in the ground state. TRIR spectra of (c) **1** and (d) **2** following photoexcitation. Figure adapted from ref. 34 with permission.

Computing excited state IR spectra and aromaticity

In order to correlate the experimental spectra with molecular structure more explicitly, we computed ground and excited state IR spectra by (TD-)DFT. Then we calculated difference spectra (S_Q state minus S_0 state) to compare to experiment. Calculating excited-state IR spectra of molecules of this size had to be done numerically over a period of several weeks. The computed spectra for **1** do not make it completely clear whether the S_Q state is more distorted than S_0, while T_1 is definitely more distorted (Figure 6a). The agreement between the computed difference spectrum and the experimental results is also only fair (Figure 6c). One explanation may be that the experimental geometry is more distorted than that given by the calculations. For **2**, on the other hand, there is a clear trend going from a complicated spectrum in S_0 to gradually simpler ones in S_Q and T_1 (Figure 6b). The computed difference spectrum is also fairly well-matched to experiment (Figure 6d).

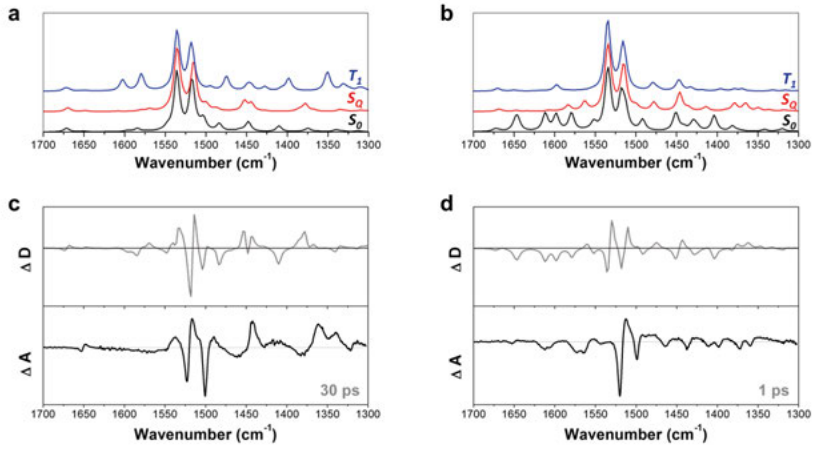

Figure 6. Simulated IR spectra for (a) **1** and (b) **2** in their S_0, S_Q and T_1 states. Comparison between calculated difference spectra (ΔD) of S_Q and S_0 and experimental absorption difference spectra (ΔA) recorded at (c) 30 ps for **1** and (d) 1 ps for **2**. Figure adapted from ref. 34 with permission.

The excited state (anti)aromatic character was probed with the geometric HOMA aromaticity index using the optimized excited-state geometries. The extent of planarization was quantified using the mean-plane deviation (MPD) and dihedral angle standard deviation (DASD). The results show gradually higher distortion and at the same time lower aromaticity for **1** going from S_0 to S_Q and T_1 (Table 1). For **2**, the trends go in the opposite direction as it becomes more planar and aromatic.

Table 1. HOMA, mean-plane deviation (MPD) and dihedral angle standard deviation (DASD) for **1** and **2** in S_0, S_Q and T_1.

	1			**2**		
	S_0	S_Q	T_1	S_0	S_Q	T_1
HOMA	0.837	0.827	0.721	0.622	0.783	0.811
MPD	0.264	0.363	0.492	0.543	0.492	0.284
DASD	5.58	6.97	12.6	14.0	11.3	5.28

Studying antiaromatic systems with TD-DFT

There are two main problems when studying ground state antiaromatic ($4n\pi$) compounds with TD-DFT: (1) presence of "invisible" low-lying doubly excited states, and (2) near-degenerate orbitals and open-shell biradical character at higher symmetries.[35] This biradical electronic structure is not possible to model with DFT, and therefore also TD-DFT fails, as it uses ground state DFT as a reference.[36] In the ground state, the molecule can often distort, lifting the orbital degeneracy. Vertical excitation from the ground state minimum is

therefore possible with TD-DFT, but optimization in the excited state can lead to a planar and bond-equalized geometry for which the ground state DFT reference fails.

Due to these two problems, the TD-DFT method cannot be used for $4n\pi$ systems unless benchmarked against multiconfigurational methods such as CASSCF. For **2**, CASSCF revealed that the experimentally studied S_Q state is actually the third excited singlet state, S_3. The S_1 state given by TD-DFT is the optically dark singly excited state, while the dark doubly excited state is not seen with TD-DFT. Luckily, the S_Q state can be studied with TD-DFT as it has singly-excited character. Additionally, the optimized S_Q structure does not have sufficient bond-length equalization that the ground state DFT reference should have problems. In conclusion, TD-DFT can be used to study **2**, which is a big advantage as the molecule is large and frequency calculations are necessary to compare to the experimental data.

Summary

In summary, the results show that the S_Q state of **1** is distorted upon excitation, likely due to antiaromaticity, while the S_Q state of **2** is planarized, likely due to aromaticity. The T_1 states show higher (anti)aromaticity than the S_Q states.

3.2 Aromaticity through space (paper II)

Homoaromaticity describes the phenomenon where cyclic conjugation extends over a saturated center, giving rise to aromatic properties.[37] The prototypical example is the homotropylium cation, which has 6 π-electrons and is homoconjugated through space. If one considers an excitation from the HOMO to the LUMO, homoconjugation should be weakened as the HOMO is C---C bonding while the LUMO is C---C antibonding (Figure 7). Conversely, the analogous compound with 8 π-electrons should have its homoconjugation strengthened.

From this qualitative picture it could be anticipated that compounds with $4n$ π-electrons capable of homoconjugation could be excited-state homoaromatic. This is also what we found in a computational study on a set of candidate structures in the T_1 excited state (Figure 8).[38]

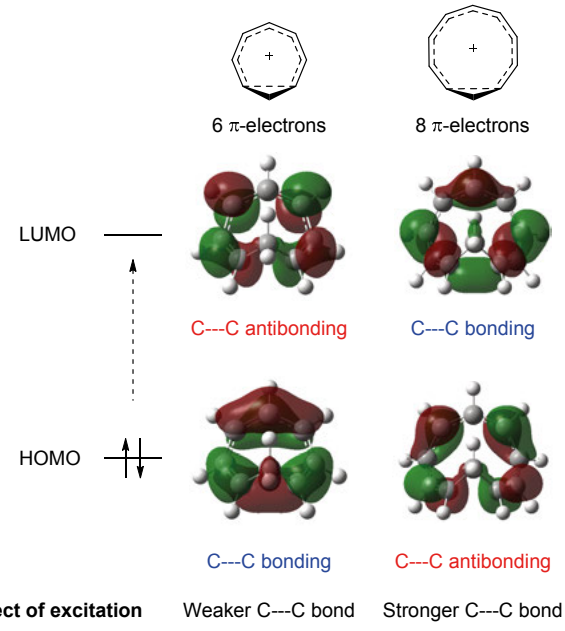

Figure 7. Effect of excitation on homoconjugated compounds with 6 and 8 π-electrons. Calculated with B3LYP/6-311+G(d,p) and 0.02 isosurface value. Figure reproduced from ref. 38 with permission.

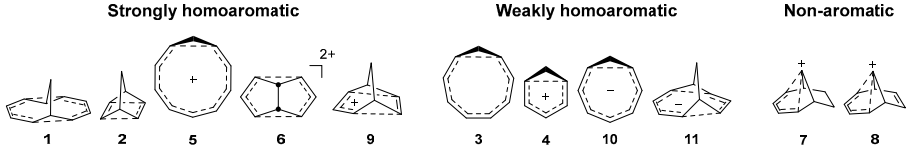

Figure 8. Investigated compounds and their extent of T_1 homoaromaticity.

Computational results

First, the geometries were optimized in T_1. Homoaromaticity is weaker than conventional aromaticity and more difficult to assess. Therefore, we used a multitude of criteria and compared the T_1 state candidates to compounds which are known to be ground state homoaromatic. Through-space conjugation was evaluated with the distance of the C---C through-space interaction (r(C---C)) and the Wiberg bond index (WBI(C---C)). The extent of delocalization was estimated with the bond-length alternation (BLA), standard deviation of atomic charge (σ_Q) and spin (σ_D) and the multicenter index (MCI). The energetic aspect was studied with the ISE method. Magnetic aromaticity was probed with ACID and NICS.

As an example, the ACID plots for selected compounds show ring currents of the same order of magnitude as in the S_0 ground state analogues and NICS scans corroborate this picture (Figure 9).

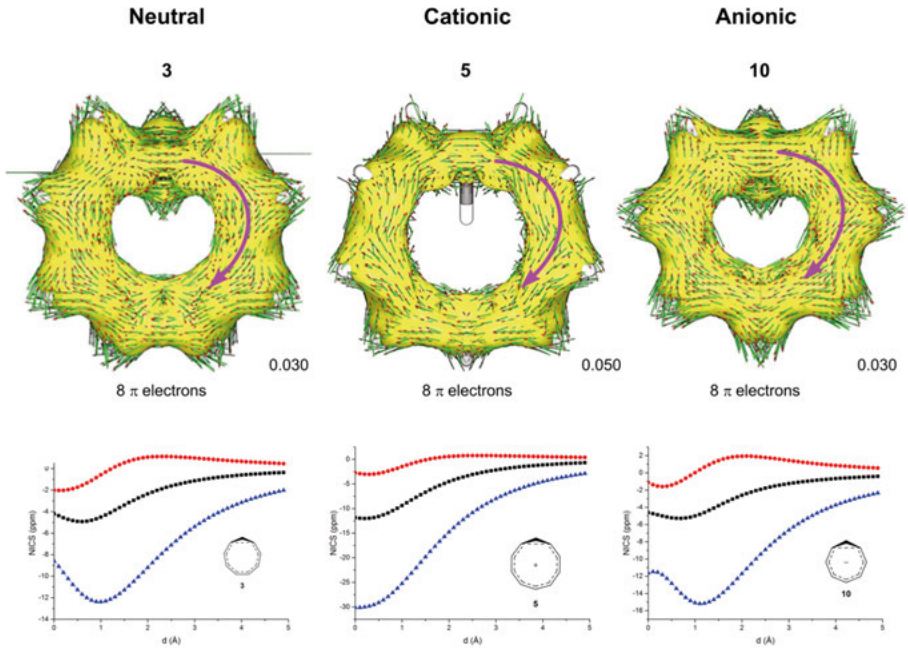

Figure 9. ACID plots and NICS scans in T_1 for selected compounds. Figure adapted from ref. 38 with permission.

The candidate compounds were evaluated against the different criteria to assess the extent of aromaticity. Five of the candidates were found to be strongly homoaromatic, four to be weakly homoaromatic and two to be non-aromatic (Figure 8).

Relevance for photochemistry

We found several photoreactions from the literature which have homoaromatic intermediates (Figure 10a) and there are likely more examples to be discovered. One of these was found during the work on this study as we investigated the norbornadiene-quadricyclane photoisomerization.[39] In this case, the homoaromatic structure is a small minimum which lies on the relaxation pathway from the vertically exited structure to the photoproduct and probably has no effect on photochemistry. Also, I used the concept to computationally design a photomechanical "lever" based on excited state antiaromaticity (Figure 10b). Following photoexcitation, the lever should swing open to avoid antiaromatic destabilization and then relax through a conical intersection back to the original position.

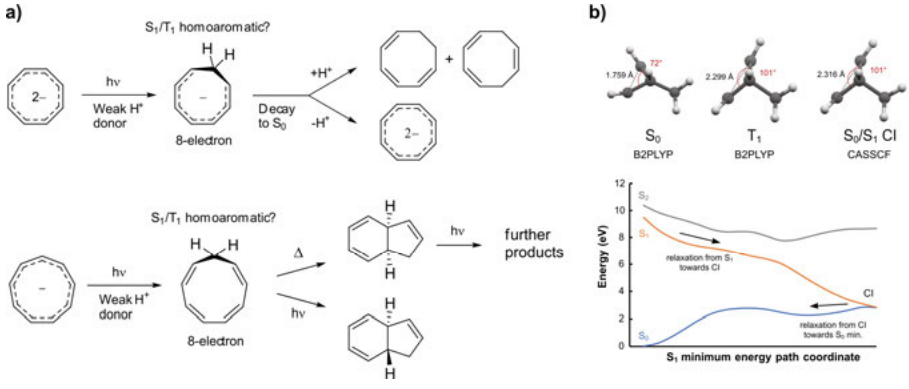

Figure 10. (a) Photoreactions from the literature with reported excited state homoaromatic intermediates. (b) Computational design of a photomechanical lever. Figure adapted from ref. 38 with permission.

Summary

Aromaticity *via* through-space conjugation, homoaromaticity, can occur in the T_1 state. This was shown by a multitude of aromaticity indices and by comparison to well-known ground state homoaromatic compounds. Preliminary results indicate that the concept should also be valid for the S_1 state.

4 Reactivity

The work presented in this chapter explores the relationship between excited state (anti)aromaticity and chemical reactivity. First, I describe how the aromatic stabilization energy in excited states was quantified experimentally for the first time. Aromatic stabilization is then related to reactivity through the Bell-Evans-Polanyi principle.[40] The validity of this principle is discussed in the context of two reactive probes suggested for experimentally determining whether a ring is excited-state aromatic (probe does not react) or antiaromatic (probe reacts). Then, two photochemical reactions which involve alleviation of excited state antiaromaticity are discussed.

4.1 Experimental quantification of aromatic stabilization (paper III)

The first experimental quantification of excited state aromatic stabilization resulted from a collaboration with the group of Prof. Aida and Dr. Itoh at The University of Tokyo.[41] Establishing the magnitude of aromatic stabilization in the excited states is very important for photochemical applications due to the close connection between stability and reactivity. Here I focus on the computational results which I contributed to the study.

Principle of quantification

Cyclooctatetraene (COT) prefers a puckered, tub-shaped conformation in the electronic ground state. This is not, as commonly believed, due to antiaromatic destabilization of the bond-length alternating planar structure, but due to strain.[42] In the excited states, this strain is overcome by aromatic stabilization and a planar, bond-length equalized structure is found (Figure 11a). In systems with higher strain, the ring inversion barrier may not be removed completely. The aromatic stabilization energy (ASE) can then be estimated as the difference of the ring inversion barriers between the ground state and the excited states (Figure 11b).

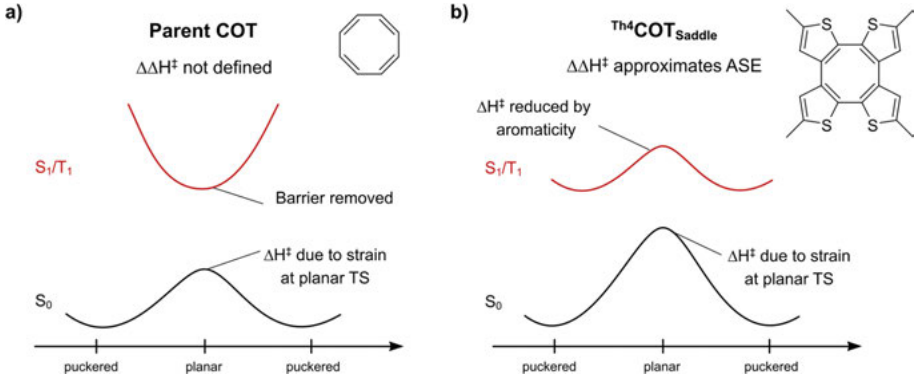

Figure 11. Principle for measuring ASE in excited states. (a) COT cannot be used as $\Delta\Delta H^{\ddagger}$ is not defined. (b) **^{Th4}COT$_{Saddle}$** is suitable as barrier remains upon excitation.

Experimental and computational results

Compound **^{Th4}COT$_{Saddle}$** was found as a byproduct of polythiophene synthesis together with its larger congener **^{Th6}CDH$_{Screw}$**. Both compounds are chiral but racemize slowly at room temperature and the rate can be followed by circular dichroism (CD) spectroscopy on enantiomerically pure samples. For **^{Th4}COT$_{Saddle}$**, ring inversion takes place via a transition state with the central COT ring planar. Activation enthalpies ($\Delta H^{\ddagger}$) were obtained via Eyring plots at different temperatures. Performing the experiment under both direct illumination and with a triplet sensitizer gave values of $\Delta H^{\ddagger}$ for S_1 and T_1. For **^{Th4}COT$_{Saddle}$**, $\Delta H^{\ddagger}$ is significantly reduced from 25.4 kcal/mol in S_0 to 4.3 kcal/mol in S_1 and 4.0 kcal/mol in T_1, respectively (Figure 12). The ASE is estimated to ca. 21 kcal/mol as the difference in $\Delta H^{\ddagger}$ between S_0 and S_1/T_1 ($\Delta\Delta H^{\ddagger}$). These values are reproduced by the calculations, with a systematic overestimation of $\Delta H^{\ddagger}$ by 4–5 kcal/mol, while $\Delta\Delta H^{\ddagger}$ is still 21 kcal/mol.

Importantly, the calculated ACID plots and NICS values show that the T_1 inversion TS is aromatic, and this is likely true also for S_1 based on the geometry and qualitative NICS scans (Figure 13). **^{Th6}CDH$_{Screw}$** served as a non-aromatic reference since its TS is not planar due to strain. Here, photoexcitation does not impact the inversion rate, suggesting that the barrier is similar or higher in the excited states, which was also supported by calculations.

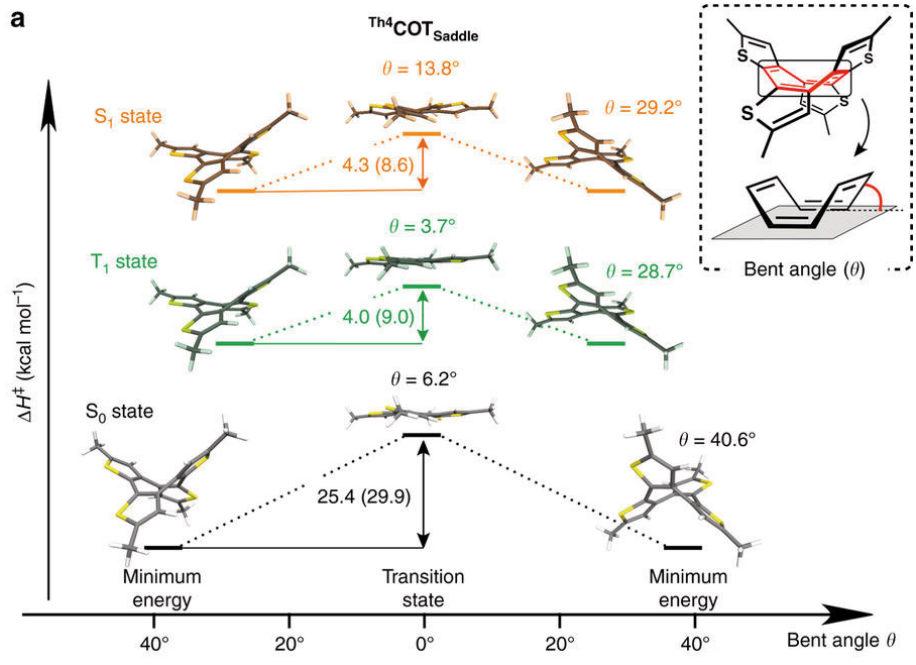

Figure 12. Experimental and computed (in parenthesis) activation enthalpies for ^{Th4}**COT**$_{Saddle}$. Figure adapted from reference 41 with permission.

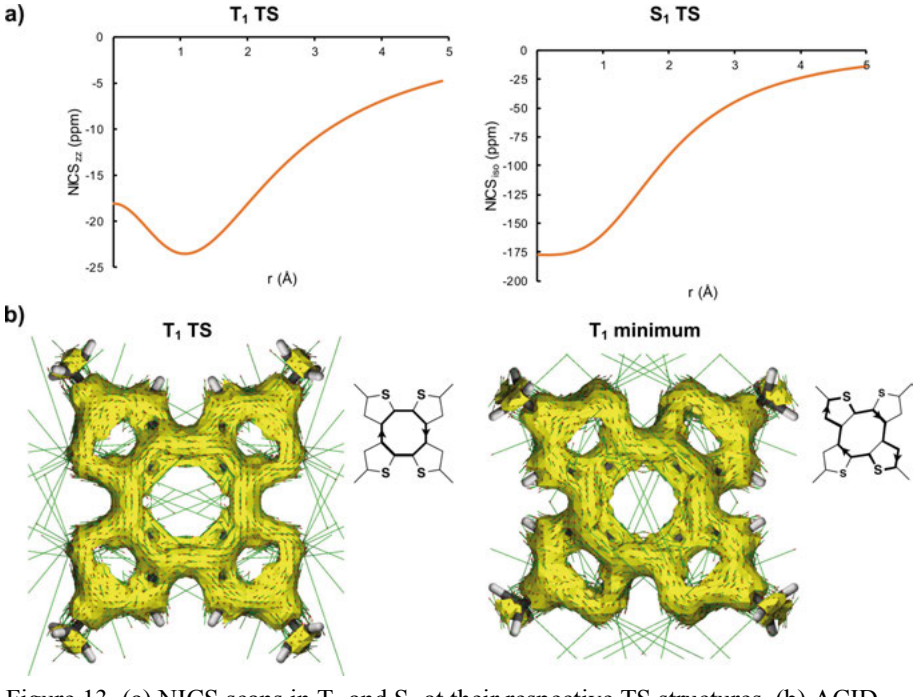

Figure 13. (a) NICS scans in T_1 and S_1 at their respective TS structures. (b) ACID plots for the TS and minimum in T_1. Insets show the dominating conjugated circuit for the ring current.

Further questions

Interestingly, the tub-shaped minimum for **^{Th4}COT$_{Saddle}$** also shows aromatic character in T_1. The ACID plot hints that 16-electron circuits are dominating the cyclic conjugation rather than the central 8-electron one (see Supporting Information of Paper III). How would this impact the quantification of ASE? If the tub-shaped structure is also stabilized by aromaticity, its energy is lower than if it was non-aromatic. The excited-state $\Delta H^{\ddagger}$ becomes higher and $\Delta\Delta H^{\ddagger}$ lower. Aromatic stabilization of the tub-shaped structure therefore leads to an underestimation of the ASE of unknown magnitude.

How is the excited state barrier affected by bond-length effects? The primary reason for the higher barrier in **^{Th4}COT$_{Saddle}$** *vs.* COT should be steric repulsion between the thiophene sulfur lone pairs and between the thiophene hydrogens. The COT C-C bonds bridging two thiophene units are shortened from 1.454/1.471 Å in S_0 to 1.404/1.428 Å in T_1 and 1.405/1.425 Å in S_1, leading to higher steric repulsion. The barrier should therefore be higher in the excited state if only steric factors were considered and the ASE will be underestimated by an unknown amount also by this effect.

Summary

The aromatic stabilization energy in the T_1 and S_1 excited states of **^{Th4}COT$_{Saddle}$** was estimated both experimentally and computationally to be ca 21 kcal/mol, based on the difference in ring-inversion barriers for the ground state and the photoexcited states. Calculation of magnetic aromaticity indices supported the aromaticity of the excited states.

4.2 Relationship between (anti)aromaticity and reactivity

Stability can be related to reactivity through the Bell-Evans-Polanyi (BEP) principle. The BEP principle[40] states that there is a relationship between the reaction enthalpy (ΔH) and the activation energy (E_a) within a family of similar chemical reactions with constant E_0 and α:

$$E_a = E_0 + \alpha\Delta H$$

Excited-state aromatic compounds should be low in energy compared to a non-aromatic product, giving a more positive ΔH and thus a high E_a (Figure 14). Excited-state antiaromatic compounds should be higher in energy, giving a more negative ΔH and thus a lower E_a (Figure 14). The influence of aromaticity on reactivity is here indirect as it is the reactant and not the transition state that is influenced by aromaticity, as it is for, *e.g.*, cycloaddition reactions.

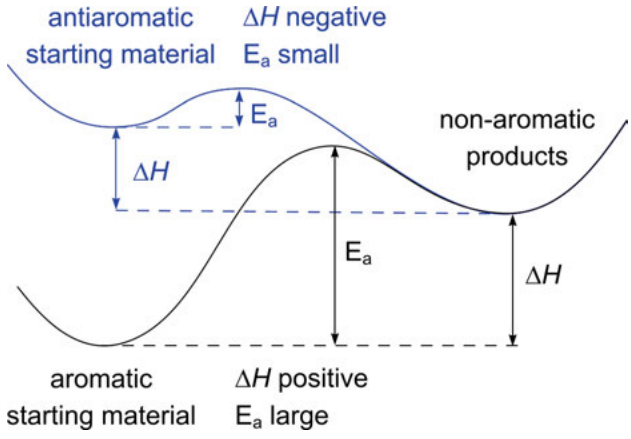

Figure 14. Bell-Evans-Polanyi principle applied to aromatic (black) and antiaromatic (blue) reactants, giving non-aromatic products.

4.3 Two reactive probes for the excited state (paper IV and V)

We tested two chemical groups that could function as reactive probes for (anti)aromaticity in excited states. The cyclopropyl group (cPr) was studied both experimentally and computationally (Figure 15a), and the silacyclobutene (SCB) unit was investigated only computationally (Figure 15b). Attachment of these structural units to a suspected excited-state aromatic or antiaromatic ring could provide an experimental aromatic diagnostic of the ring in question. Excited-state antiaromatic rings should open up the reactive probes with a smaller activation energy than the excited-state aromatic rings according if the reaction follows the BEP princple (Figure 15c). Here I focus on the calculations which I was involved in.

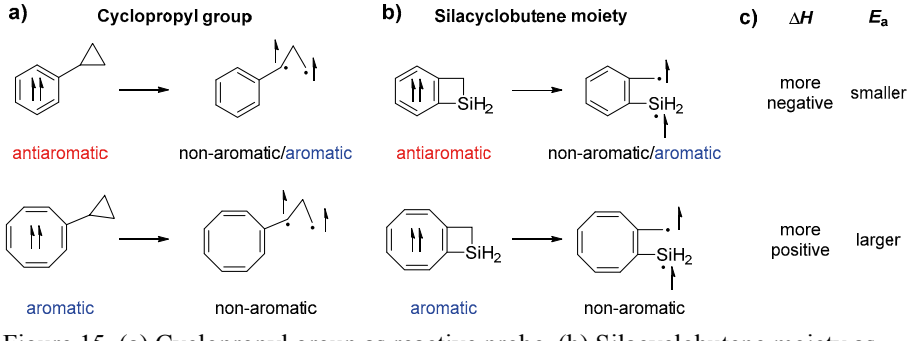

Figure 15. (a) Cyclopropyl group as reactive probe. (b) Silacyclobutene moiety as reactive probe. (c) Bell-Evans-Polanyi analysis of activation energies with respect to non-aromatic reactants as reference.

Cyclopropyl group

The cPr group is a well-established radical clock which opens when attached to a radical center.[43] We investigated if this would happen also in the T_1 excited state, which has biradical character. Opening of the ring shifts the localization of the triplet excitation from the annulene, with one unpaired electron residing on the annulene and one as an alkyl radical (Figure 15a). The reactants are (anti)aromatic while the products are mainly non-aromatic. If the reaction follows the BEP principle, the activation energy should be governed by the reaction energy and therefore be lower for excited-state antiaromatic annulenes as compared to aromatic ones (Figure 15c). We investigated the activation energies in T_1 of a series of all-carbon and heterocyclic compounds, both non-aromatic and those with $4n$ and $4n + 2$ π-electrons (Figure 16).

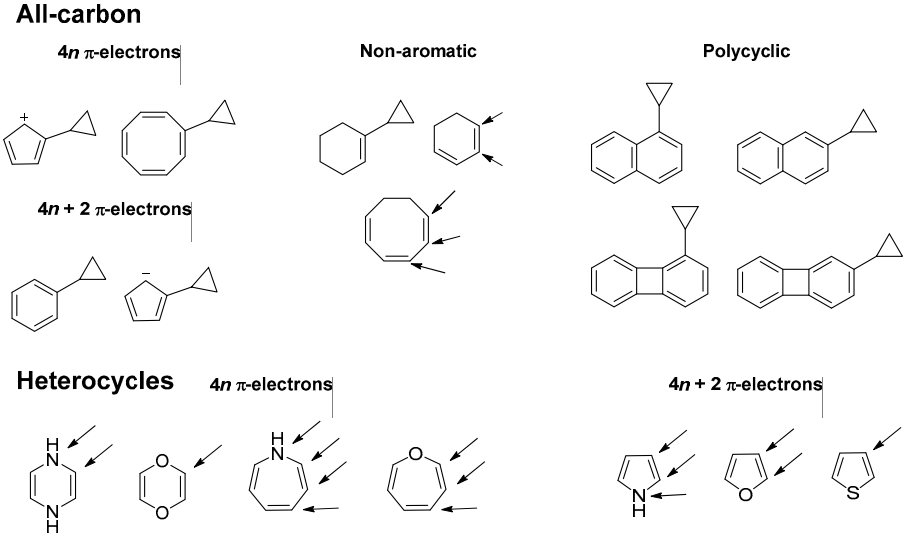

Figure 16. Investigated compounds with cPr group substitution indicated by arrows when applicable. Only monosubstituted compounds were considered.

DFT calculations for the monocyclic all-carbon compounds showed that the BEP principle is followed approximately (Figure 17) with high activation energies shown for T_1 aromatic compounds ($4n$) and low activation energies shown for T_1 antiaromatic compounds ($4n + 2$). The spread is quite large for the non-aromatic compounds, which can be explained by the positioning of the cPr group, as higher activation energies are obtained if the spin density at the cPr-substituted atom is lower. This additional factor complicates the BEP analysis, which is nevertheless still qualitatively valid. ACID plots and HOMA values confirmed the changes in aromaticity during the reaction. CASSCF calculations on benzene and COT showed that the results can likely be extended to the S_1 state.

Experimentally, cPr-benzene was reactive with irradiation at 254 nm in methanol, eventually forming polymers, while only starting materials were recovered for cPr-COT under direct or sensitized irradiation. cPr-substituted polycyclic compounds such as naphthalene and biphenylene showed more complicated behavior. Experimentally, the reacting state (S_1 vs T_1) and the excited state lifetime are complicating factors that need to be considered on a case-by-case basis.

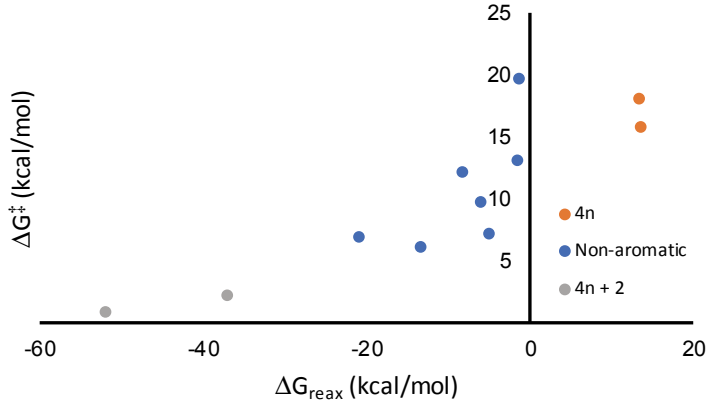

Figure 17. Relation between reaction free energy and activation free energy in T_1 for cPr-substituted all-carbon aromatic, non-aromatic and antiaromatic compounds.

For the heterocyclic compounds, where the heteroatom contributes a lone pair to the conjugation, there are also some complicating factors. One of these is the presence of several heteroatoms and another is when the cPr group is attached directly to the heteroatom. When these more complicated cases are excluded, a fair relation between the reaction energy and activation energy is seen (Figure 18). Again, the spin density is a factor not taken into consideration which induces a significant spread in the activation energies. CASSCF calculations on two of the compounds indicated that the results could be extended to the S_1 state.

Silacyclobutene moiety

The SCB unit is another candidate for an (anti)aromaticity probe which works by opening the ring in an electrocyclic reaction (Figure 15b). The triplet excitation is transferred from the annulene to the new alkyl and silyl radical centers, transforming the annulene from (anti)aromatic to (non-)aromatic. The reaction free energies (ΔG_r) and activation free energies ($\Delta G^{\ddagger}$) were calculated for a series of aromatic, antiaromatic and non-aromatic candidates using DFT (Figure 19).

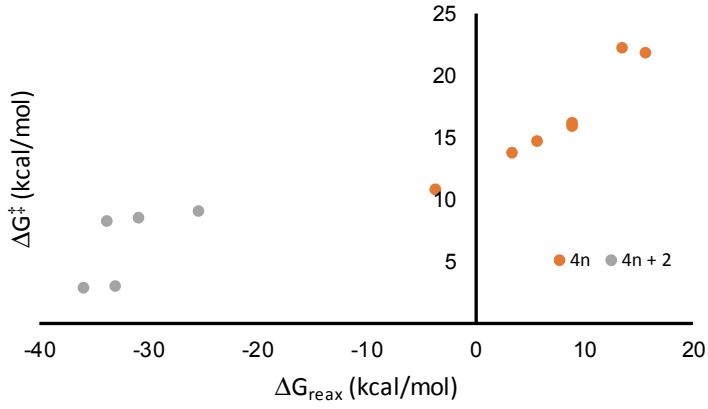

Figure 18. Relation between reaction free energy and activation free energy for T_1 aromatic and antiaromatic heterocyclic compounds.

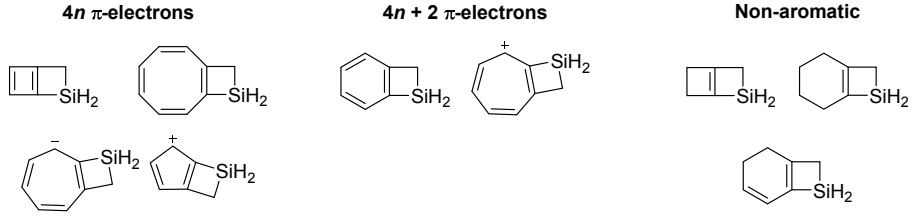

Figure 19. Investigated compounds with SCB units.

The results show that the T_1-aromatic compounds have significantly larger $\Delta G^{\ddagger}$, while antiaromatic and non-aromatic compounds have lower $\Delta G^{\ddagger}$. The BEP principle is approximately followed (Figure 20). Cyclobutadiene is an outlier with a high $\Delta G^{\ddagger}$ despite the low ΔG_r. This behavior is likely due to the high ring strain in the small four-membered ring. Like the cPr substituent, the SCB moiety cannot distinguish between non-aromatic and antiaromatic rings as both have activation energies in the reactive range. Only the T_1-aromatic units are predicted to remain closed under irradiation.

Aromaticity analysis using HOMA, NICS and ACID confirmed that the reaction proceeds from (anti)aromatic reactant to (non-)aromatic products. Comparison between the compounds in S_0 and T_1 reveal similar trends, showing that aromaticity is governing the activation energy in an analogous way in both states (Figure 21).

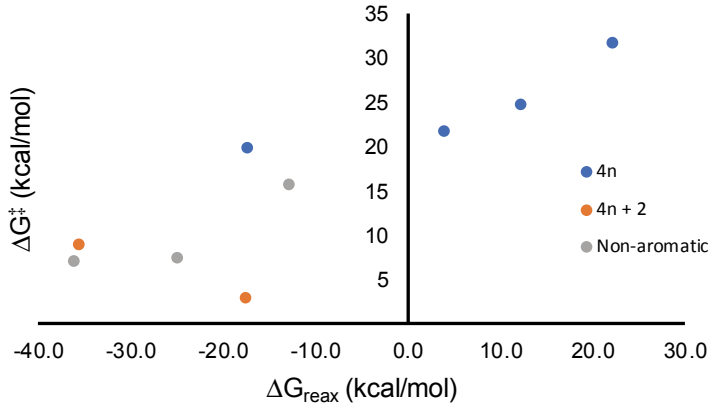

Figure 20. Relation between reaction free energy and activation free energy for T_1 aromatic, non-aromatic and antiaromatic compounds.

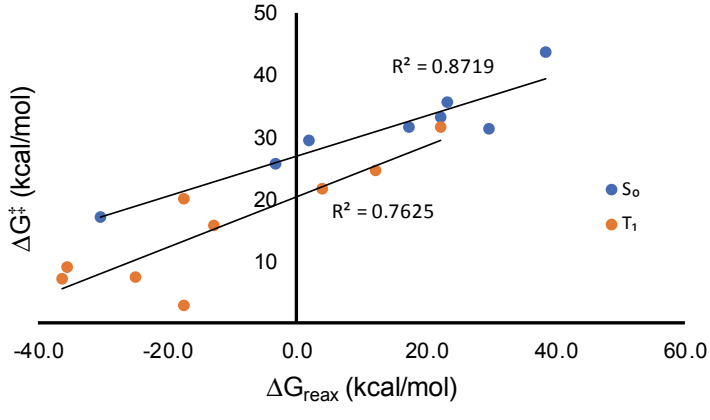

Figure 21. Relation between reaction free energy and activation free energy for compounds in the S_0 and T_1 states.

Summary

The results support that excited state (anti)aromaticity affects reactivity in accordance with the BEP principle. The cPr and SCB moieties could be used as indicators for excited state aromaticity in T_1 and possibly also in S_1. However, they cannot discriminate between non-aromatic and antiaromatic compounds which have activation energies in the reactive range. There are limitations in polycyclic systems and systems with many heteroatoms whose lone pairs are part of the cyclic conjugation. Also, the attachment point of the probes with respect to the T_1 spin density will affect the barrier heights.

4.4 Cyclization of enynes to benzofulvenes (paper VI)

Our collaborators in the group of Prof. Alabugin at Florida State University discovered that benzannelated enynes could be photochemically converted to benzofulvenes with release of formaldehyde (Figure 22).[44] Direct irradiation at 300 nm generally gave a mixture of benzofulvene and naphthalene products. The formation of benzofulvenes was found to occur in the triplet excited state as the yields are dramatically increased in the presence of a triplet sensitizer. The formation of naphthalenes is believed to occur through the singlet excited state which is the state reached by direct irradiation. Some substituted substrates gave only benzofulvenes even without sensitization, and it is likely that they have efficient inter-system crossing to the T_1 state after excitation.

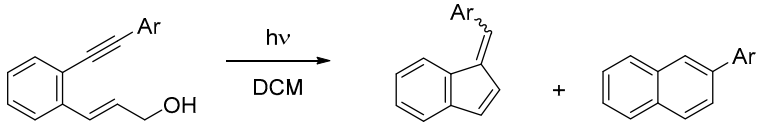

Figure 22. Photochemical formation of benzofulvenes from benzannelated enynes with naphthalene byproduct.

Computational investigation of mechanism

We investigated the reaction mechanism computationally, starting from the triplet excited state of the enyne (Figure 23). The relaxed structure shows a twisted exocyclic double bond and the triplet state therefore behaves like two mainly non-interacting alkyl and benzyl radicals. In the next step, the alkyl radical attacks the alkyne in a 5-exo-dig/5-endo-trig fashion to close the five-membered ring. Further reaction in the T_1 state with loss of formaldehyde has a prohibitively high barrier of 17.4 kcal/mol. Instead, inter-system crossing to the S_0 state should occur efficiently as the energy gap is only 1.4 kcal/mol. Now, concerted loss of formaldehyde and H-atom abstraction leads to the product with a barrier of only 10.3 kcal/mol. DFT functional dependence was small as good agreement was obtained with M06-2X and OLYP.

Role of excited state antiaromaticity

The central benzene ring of the vertically excited enyne is antiaromatic according to ACID and NICS (Figure 24). Relaxation leads to the terminally twisted minimum where the ring instead is weakly aromatic with ACID plots and NICS values which are similar to the benzyl radical.

Experimentally, it was found that a non-aromatic enyne substrate did not react (Figure 23a). Computations revealed the likely reason to be a higher activation energy (12.6 kcal/mol) of the initial cyclization step. The reason for this higher barrier is the presence of a planar conformation which lies 6.3 kcal/mol below the terminally twisted one. This energy difference is very similar to the 5.6 kcal/mol difference in activation energy between non-aromatic

and aromatic substrates (Figure 23b), meaning that if they start from the twisted conformation, both substrates are equally reactive.

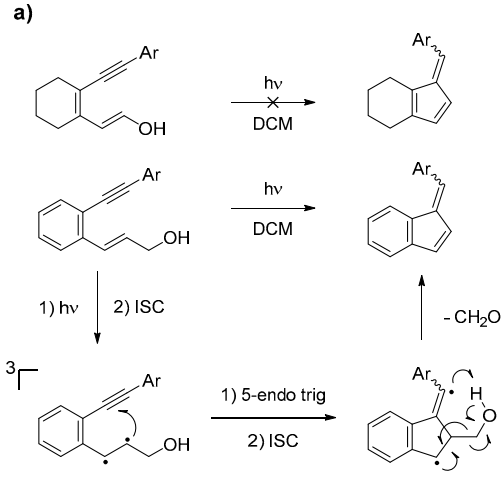

b)

Starting material	Computed barriers	
	S_0	T_1
non-aromatic	37.3	12.6
aromatic	41.1	7.0

Figure 23. (a) Proposed reaction mechanism. (b) Comparison between activation energy of ring-closure for non-aromatic and aromatic substrates (in kcal/mol).

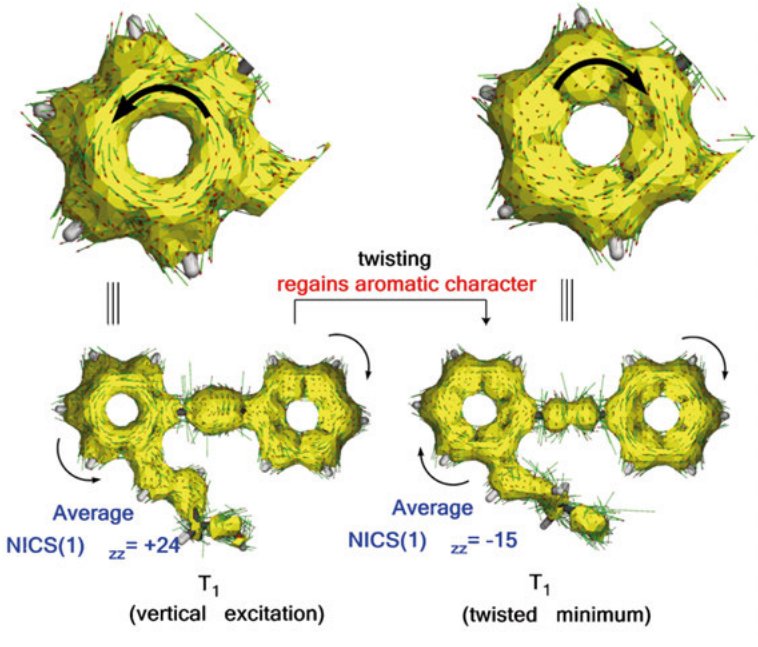

Figure 24. ACID plots and NICS values showing antiaromatic character of vertically excited benzene ring and aromatic character of the twisted minimum. Figure adapted from ref. 44 with permission.

The influence of antiaromaticity can therefore be seen as "pushing" the triplet excitation onto the exocyclic double bond by destabilizing the planar conformation. The magnitude of destabilization can be estimated to 14.8 kcal/mol from the energy difference between the twisted and planar structure for the non-aromatic (6.3 kcal/mol) and aromatic substrates (-8.5 kcal/mol, computationally constrained). This value is in line with computational estimates of the antiaromatic destabilization of T_1 benzene at 16.9 kcal/mol.[25c]

Summary

Benzannelated enynes can be converted photochemically to benzofulvenes in the T_1 state, while non-aromatic substrates were unreactive. The difference in reactivity is attributed to T_1-state antiaromaticity in the benzannelated species, favoring the reactive conformation with a twisted exocyclic double bond.

4.5 Hydrogenation and hydrosilylation of small PAHs and graphene (paper VII)

Hydrogenation energies of annulenes calculated with DFT show a zig-zag dependence on the number of π-electrons, with 4*n* annulenes being easier to hydrogenate and 4*n* + 2 annulenes being more difficult (Figure 25).[45] In accordance with Baird's rule, this trend is reversed in the T_1 excited state, where ground state aromatic compounds should be easier to hydrogenate.

Calculated magnetic properties using ACID plots (Figure 26) and NICS-XY scans (Figure 27) showed that also polycyclic aromatic hydrocarbons (PAHs) are antiaromatic in their T_1 states, with the paratropic ring currents localized more in certain rings. From these computational results it can be anticipated that photochemical hydrogenation of benzene and PAHs should be more facile than the thermal reaction.

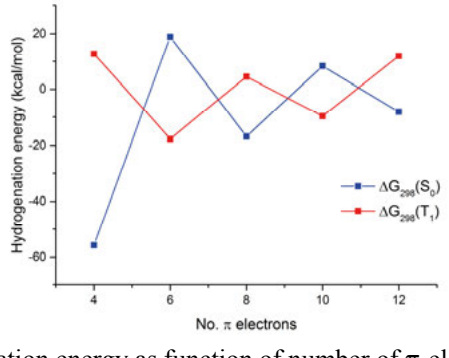

Figure 25. Hydrogenation energy as function of number of π-electrons for the S_0 and T_1 states. Each point is an average of several compounds with the same number of π electrons. Figure adapted from ref. 45 with permission.

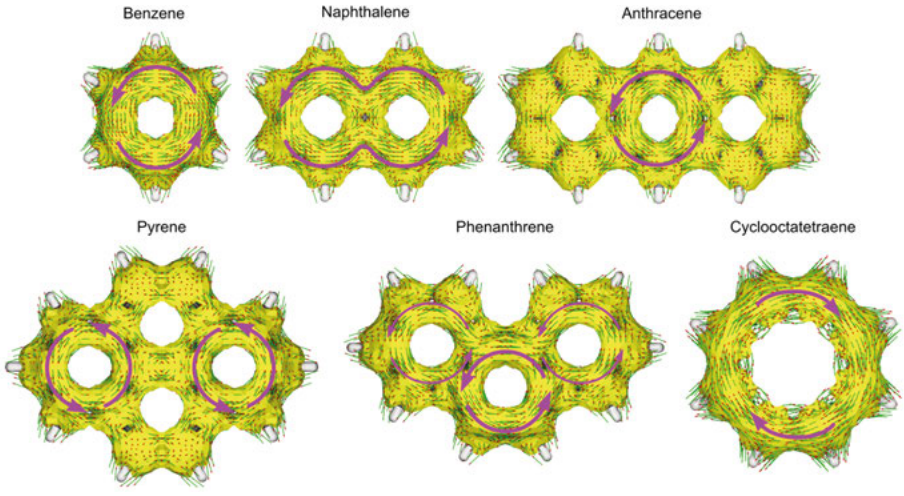

Figure 26. ACID plots of benzene, polycyclic aromatic hydrocarbons and cyclooctatetraene in T_1. Figure adapted from ref. 45 with permission.

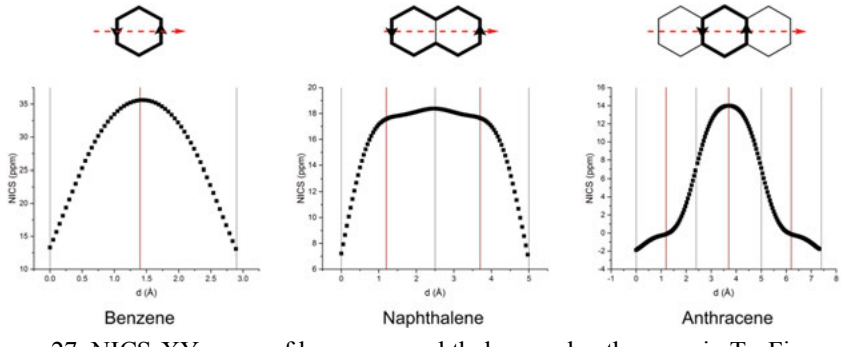

Figure 27. NICS-XY scans of benzene, naphthalene and anthracene in T_1. Figure adapted from ref. 45 with permission.

Calculations on mechanism

The reaction was carried out experimentally with Et_3SiH as a "fat" hydrogen atom donor (as use of H_2 was considered too dangerous). Our mechanistic hypothesis was that the first and rate-limiting step of the reaction is H-atom abstraction from Et_3SiH by the excited state annulene (Figure 28a). This step should occur in the T_1 state due to the facile intersystem crossing of benzene and PAHs and the longer excited-state lifetime of T_1 compared S_1.

The calculated activation energies increase from benzene (2.4 kcal/mol) to naphthalene (13.1–18.5 kcal/mol), and the larger PAHs phenanthrene (15.5 kcal/mol), anthracene (19.2 kcal/mol) and pyrene (28.1 kcal/mol). For excited-state aromatic COT the barrier is much higher at 35.9 kcal/mol. The calculated barrier for benzene in the S_1 state at 27.2 kcal/mol is too high to allow reaction, supporting the hypothesis that the reaction goes through the T_1 state.

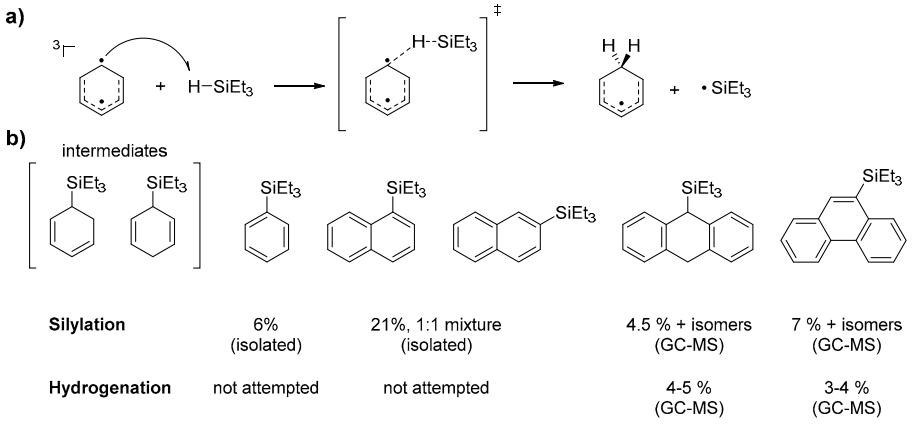

Figure 28. (a) Mechanistic hypothesis for rate-determining step of photosilylations. (b) Products with yields for silylation and hydrogenation.

Experimental results

The trends in computed activation energies were reflected in the experimental reactivity where benzene is highly reactive, naphthalene, anthracene and phenanthrene react slower, while pyrene, fluoranthene and coronene were (almost) unreactive (Figure 28b). In accordance with its excited-state aromatic character, COT was also unreactive.

Finally, it was shown that graphene could be both photohydrogenated and photohydrosilylated. How this relates to a potential antiaromatic character of photoexcited graphene is not clear. Graphene is an extended material and therefore it is hard to directly apply molecular concepts such as aromaticity, although interpretations have been made.[45,46] One possibility is that the photoreactions occur at defects which behave more like PAHs.

Summary

Benzene and PAHs undergo photochemical hydrosilylation and transfer hydrogenation. This reactivity is consistent with their T_1 antiaromaticity and that the computed hydrogenation energies are lower in the excited state. Even graphene was reactive upon irradiation, but the relation to excited-state antiaromaticity is not clear.

5 Properties

In this chapter I focus on the influence of aromaticity on molecular properties. Could aromaticity be used as a design principle to tune excited state energies and even create molecules which have triplet ground states? This idea is based on that aromatic compounds generally have high-lying excited states while those for antiaromatic are low-lying.[7] First we look at siloles and cyclopentadienes, for which excitation energies can be tuned by substitution.[47] We then explore how to design polycyclic systems which are both stable and have low triplet energies.[48] Finally, we look at a proposed design that does not give low excited state energies but is nonetheless fundamentally interesting as it gives Hückel-Baird hybrid compounds.[49]

5.1 Qualitative model for substituent effects in siloles and cyclopentadienes (paper VIII)

It was previously shown that fulvenes could act as "aromatic chameleons" that adapt their electronic structure to the rules for aromaticity in the S_0 ground state as well as the S_1 and T_1 states (Figure 29a).[50] This chameleon behavior is made possible by the influence of dipolar resonance structures with either a positive or a negative charge on the five-membered ring. The weight of these resonance structures can be enhanced by electron-withdrawing groups (EWGs) and electron-donating groups (EDGs) on the exocyclic double bond. According to the isolobal analogy,[51] cyclopentadienes and siloles should show similar behavior as their formally saturated EX_2 unit (E = C, Si) can hyperconjugate with the butadiene π system in the same fashion as a C=C double bond (Figure 29b). However, this interaction – called *cross-hyperconjugation*[52] – should be weaker than in the fulvenes.

Previously, the absorption properties of siloles have been interpreted in terms of the σ^*-π^* model, in which the key interaction is a lowering of the LUMO due to interaction between a π^* orbital on the butadiene fragment and a σ^* orbital on the SiR_2 fragment (Figure 29c).[53] The qualitative model based on aromaticity/antiaromaticity effects presented here is an alternative viewpoint.

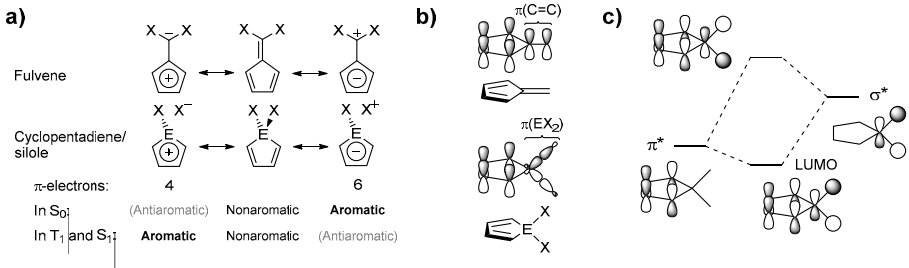

Figure 29. (a) Fulvenes and siloles/cyclopentadienes as aromatic chameleons. (b) Isolobal analogy. (c) σ*-π* model for siloles.

Influence of aromaticity on excitation energies

The aromatic chameleon behavior opens a way to rationally tune excitation energies by substitution (Figure 30). With EWGs, the ground state is mainly non-aromatic as the molecule tries to avoid antiaromaticity by favoring the quinoid resonance structure. In the excited state, the polar resonance structure with 4 π-electrons and a positive charge on the ring is favored. Excitation occurs from a non-aromatic ground state to an aromatic excited state and the excitation energy should therefore be low. The excitation should also be accompanied by a change in dipole moment as charge is being shifted. For EDGs, the excitation energy should be higher as excitation occurs from an aromatic ground state to a mainly non-aromatic excited state while the dipole moment change should still be in the same direction as for EWGs.

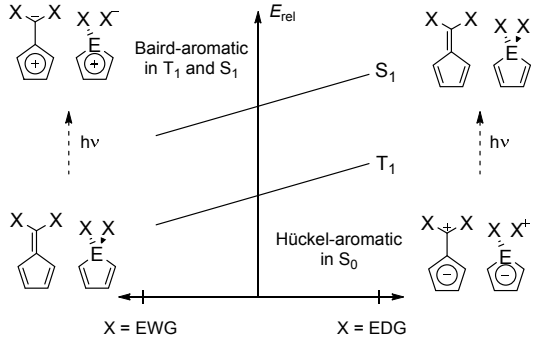

Figure 30. Effect of substitution on excitation energies of fulvenes, cyclopentadienes and siloles.

Adiabatic triplet excitation energies (ΔE_{ST}) were calculated with DFT and correlated to four indices that cover different aspects of aromaticity: NICS (magnetic), HOMA (geometric), ISE (energetic) and Shannon aromaticity (electronic). The very good linear relations between ΔE_{ST} and all indices strongly support the notion that aromaticity changes are intimately connected to the excitation energies (Figure 31a). The dipole moment changes were also consistent with the proposed model. As expected from the electron counting rules,

switching to three- or seven-membered rings switched the effect of EWGs and EDGs and the direction of the dipole moment change upon excitation as the number of electrons in the rings changed by ± 2. A literature survey also showed that the model was consistent with published experimental data on singlet excitation energies (Figure 31b).

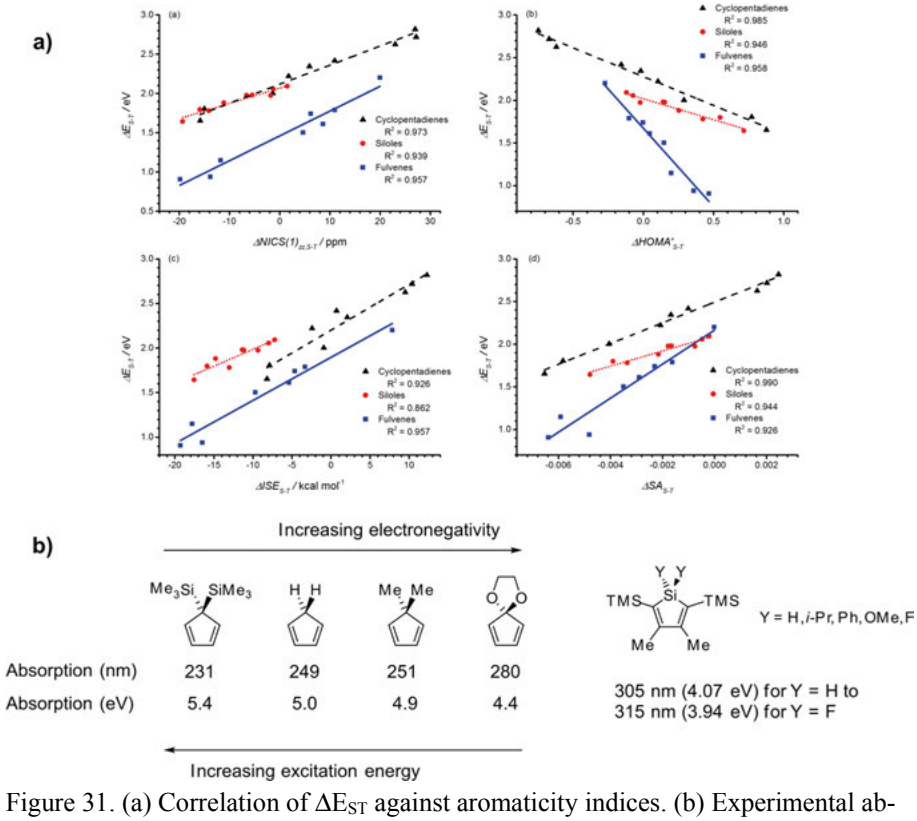

Figure 31. (a) Correlation of ΔE_{ST} against aromaticity indices. (b) Experimental absorption energies of cyclopentadienes and siloles.

Summary

A qualitative model of cyclopentadienes and siloles as cross-hyperconjugated aromatic chameleons can be used to explain and predict changes in excitation energies upon substitution with EWGs and EDGs. Based on their higher potential for tunability and relatively low excited-state energies with EWGs, cyclopentadienes could be interesting to explore for organic electronic materials, *e.g.*, in polymers.

5.2 Combining Clar's and Baird's rules (paper IX)

Ground state antiaromatic compounds have desirable properties for organic electronic materials. These include small band-gaps, non-linear optical behavior and ambipolar electron transport of either electrons or holes.[54] In their triplet states they are instead stabilized and could find use in spintronics devices.[55]

Unfortunately, these types of molecules are generally very unstable and difficult to synthesize. For example, the parent cyclobutadiene and pentalene can only be prepared under matrix isolation conditions (Figure 32a).[2] However, larger analogues such as indenofluorenes with special bulky protecting groups can be prepared and retain some of their antiaromatic character. These larger analogues are often obtained by fusing benzene rings to an antiaromatic skeleton; e.g., indenofluorenes can be seen as a 12-electron indacene unit with two terminally fused benzene rings (Figure 32a). It seems that fusion with benzene rings is good strategy for stabilizing antiaromatic compounds, while still retaining many of their most desirable properties.

In this work, we focused on the triplet excited state properties and investigated how the triplet energies varied with the number and position of fused benzene rings. The ultimate goal is to find a connectivity that gives the lowest triplet energy (ΔE_{ST}) and ideally a triplet ground state.

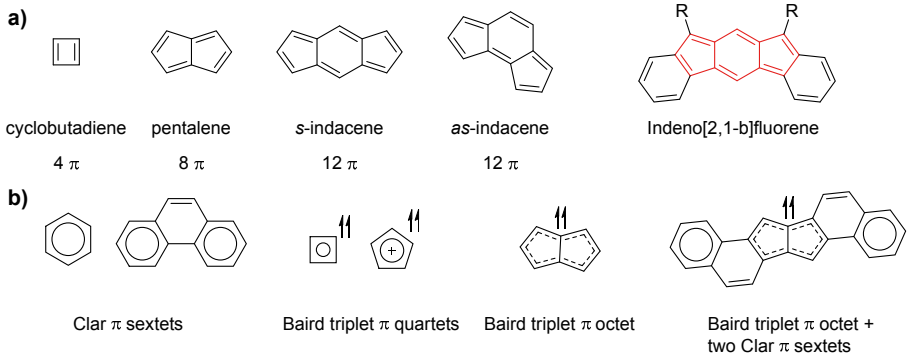

Figure 32. (a) Ground state antiaromatic compounds. (b) Clar sextets and Baird quartets/octets.

Combining Clar sextets and Baird quartets and octets

Clar's rule states that the resonance structure of a polycyclic aromatic hydrocarbon (PAH) for which one can draw the highest number of *disjoint* (isolated) π sextets is most representative of the properties of the molecule (Figure 32b). Additionally, the most stable member within a family of PAH isomers is also the one with the most π sextets.[2] We combined Clar's rule with Baird's rule,[48] and introduced the concept of *Baird quartet* and *Baird octet* to describe a disjoint 4- or 8-electron cycle with a triplet electronic configuration. A triplet state molecule can thus only have one Baird quartet/octet. The hypothesis was

that the lowest triplet energy should be obtained for those isomers that in their T_1 states have both the most number of Clar sextets and Baird quartets/octets.

The most promising compounds in the study combined a central antiaromatic unit capable of hosting a Baird quartet/octet with benzene fusion in such a way that four Clar sextets could be drawn (Figure 33a).

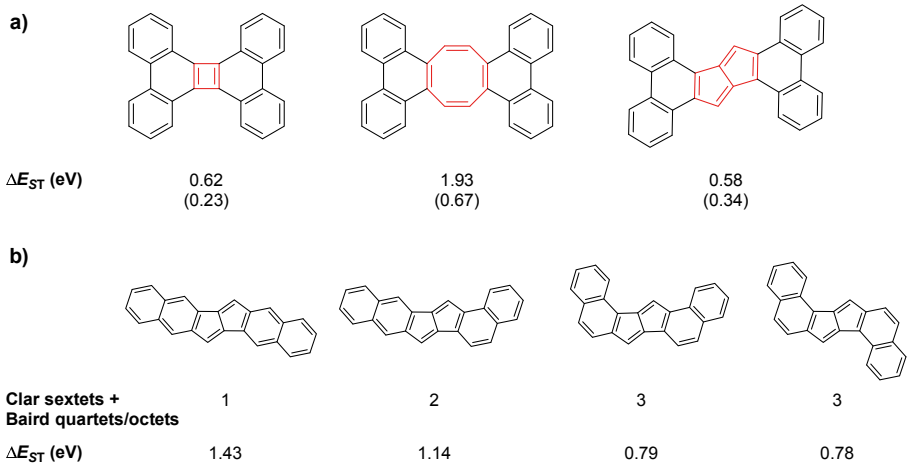

Figure 33. (a) Isomers with maximum number of sextets and quartets/octets which also displayed the lowest triplet energies. Values for parent compounds (marked in red) in parenthesis. (b) Variation of triplet energy with the combined number of sextets and quartets/octets.

The cyclobutadiene and pentalene analogues showed ΔE_{ST} values approaching those of the parent compounds, while the COT analogue displayed a considerably higher value than its parent. The presence of the quartet/octet and sextets were confirmed with several aromaticity indices, including ACID plots, NICS-XY scans, HOMA and FLU as well as spin density maps (see Figure 34 for one example).

The high ΔE_{ST} value for the COT analogue can be attributed to a steric clash between the hydrogens on the COT ring and the benzene rings, preventing the compound from attaining a planar conformation in the triplet state. Triplet energies generally decreased with the combined number of Clar sextets and Baird quartets/octets in a series of isomers (Figure 33b).

Summary

Compounds with low triplet energies can be obtained by benzannelation of antiaromatic units in such a way as to maximize the number of Clar sextets and Baird quartets/octets. The combination of Clar's and Baird's rule is therefore a possible conceptual tool for designing new compounds with low-lying triplet states.

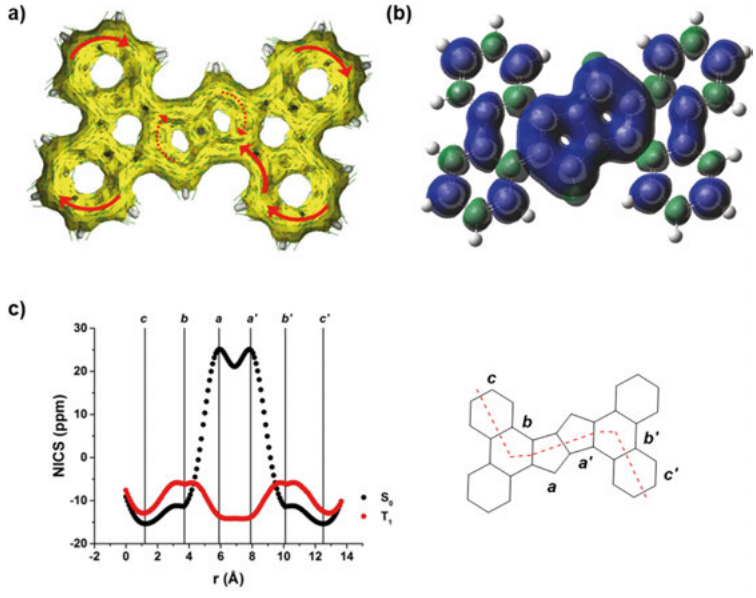

Figure 34. (a) ACID plot, (b) spin density map and (c) NICS-XY scan for tetra-benzene-fused pentalene. Figure reprinted from ref. 48 with permission.

5.3 Hückel-Baird hybrids (paper X)

Pro-aromatic compounds have one or several rings which become aromatic if a π bond is broken, and the bonds of the molecule are re-shuffled (Figure 35).[54] The energetic cost for breaking the bond is paid by aromatic stabilization of the rings and/or stabilization of the two unpaired electrons by radical-stabilizing groups. Pro-aromatic compounds can thus have open-shell character even in their ground states, and the singlet and triplet state often lie close in energy as they differ only in the spin of one electron.

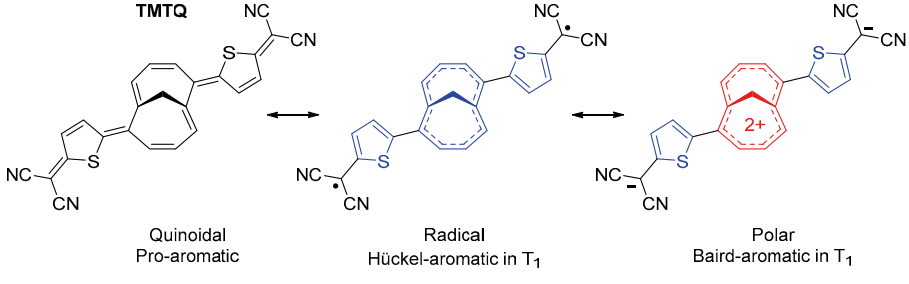

Figure 35. The pro-aromatic molecule **TMTQ** with its quinoidal, radical and polar resonance structures. Hückel-aromatic rings are shown in blue, Baird-aromatic rings in red, and non-aromatic rings in black.

Based on the small ΔE_{ST} of the molecule **TMTQ** (Figure 35), it has been suggested that another mode of stabilization of the triplet than that just described could be possible.[56] This stabilization mode is based on Baird aromaticity and involves a polar resonance structure where two electrons are removed from the central 1,6-methano[10]annulene (M10A) unit (Figure 35). The unpaired same-spin electrons of the triplet **TMTQ** are then centered on this ring, which is 8 π-electron Baird-aromatic. The conventional radical structure instead has a Hückel-aromatic central ring while the unpaired same-spin electrons are on the exocyclic carbons.

Assessing Baird vs. Hückel aromaticity

We established three criteria for assessing if the M10A unit in triplet state **TMTQ** is Baird-aromatic or Hückel-aromatic. First, if the polar structure is dominant, the M10A ring should carry a large positive charge. Second, the spin density should be localized mainly on the M10A unit for it to have a triplet electronic configuration. Third, the electron delocalization should be of Baird-type rather than Hückel type. Comparison was made to the totally Baird-aromatic triplet 1,6-methano[10]annulene dication (**M10A**$^{2+}$, Figure 36).

To assess the amount of charge transfer, we split the molecule into different fragments and summed the calculated atomic charges for each fragment. Our DFT calculations showed that the charge on the M10A unit was low and smaller in the T_1 state than in S_0 (Figure 36). This was opposite to what is expected if the polar resonance structure is more important in T_1. The results were also corroborated with charges from CASSCF and CC calculations.

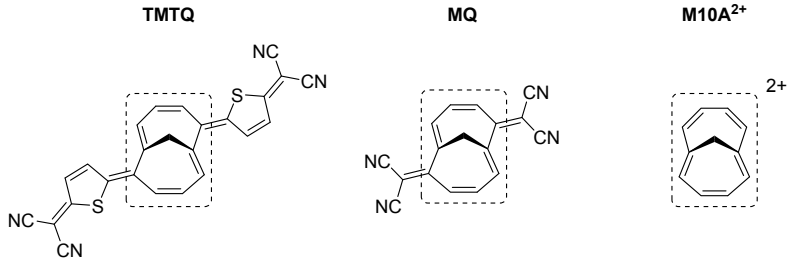

	TMTQ	MQ	M10A^{2+}
Charge	+0.240 (12%)	+0.502 (25%)	+2 (100%)
Spin density	0.257(13%)	0.684 (34%)	2 (100%)
ΔFLU/FLU	-0.2233 (11%)	-0.9113 (46%)	-2.0005 (100%)

Figure 36. Computed charge, spin and ΔFLU/FLU values for the the M10A unit in **TMTQ**, **MQ** and **M10A**$^{2+}$.

For the spin density we used the same fragments but instead summed the atomic spin densities. As the spin density of the central M10A unit of **TMTQ** is low (ca 10%), it cannot have any major Baird aromaticity.

To assess more directly whether the ring is Hückel-aromatic or Baird-aromatic, we divided the FLU aromaticity index into contributions from α and β electrons. For a Hückel-aromatic cycle with equal number of electrons of both spins, the normalized difference between FLU_β and FLU_α ($\Delta FLU/FLU$) should be zero. For a Baird-aromatic cycle, $\Delta FLU/FLU$ should be non-zero as there is an excess of α electrons. The calculated values for the M10A ring shows a small $\Delta FLU/FLU$ value which points to Hückel- rather than Baird-aromaticity.

All these calculations indicate that **TMTQ** in the T_1 state is not influenced to any large extent by Baird aromaticity and rather behaves as a conventional pro-aromatic compound.

Aromatic hybrids

While **TMTQ** is mainly Hückel-aromatic in T_1, it is possible that it has some Baird-aromatic character if the triplet state is a resonance hybrid between the radical (major) and polar (minor) resonance structures. To further explore this hypothesis, we studied the smaller compound **MQ**, which is obtained from **TMTQ** by removing the thiophene rings (Figure 36). **MQ** displays higher positive charge and spin density on the M10A unit, as well as a larger $\Delta FLU/FLU$ value, which is all consistent with higher Baird-aromatic character. At the same time, **MQ** also has a higher ΔE_{ST} of 18.5 kcal/mol as compared to 5.0 kcal/mol for **TMTQ**.

Based on these results, we proposed that there should be a continuum between the Baird- and Hückel-aromatic forms and for this we coined the term *Hückel-Baird hybrids*. **TMTQ** lies towards the Hückel-side of this continuum while **MQ** could have higher Baird-aromatic character. However, higher Baird-aromatic character leads to a higher rather than a lower ΔE_{ST}. Baird aromaticity is therefore not responsible for any unusually high stabilization in **TMTQ** and increase of Baird-aromatic character does in this case not seem like a good strategy to obtain a low triplet energy.

Summary

Hückel-Baird hybrids are compounds which in their T_1 states can be described as resonance hybrids between a diradical, Hückel-aromatic form and a polar, Baird-aromatic form. For the compound **TMTQ**, the amount of Baird character is small, at most 10%. More Baird character seems to lead to a higher ΔE_{ST} rather than a lower.

6 Conclusions and outlook

In the introduction, I asked if the concept of aromaticity as applied to photoexcited molecules could be used to explain and predict three central aspects of their behavior: structure, reactivity and properties. In this thesis I have shown that:

- Aromatic and antiaromatic molecules change their *structure* upon excitation in such a way that they gain aromatic stabilization (planarize, enable through-space conjugation) or avoid antiaromatic destabilization (pucker).
- Aromaticity and antiaromaticity are directly related to *reactivity* via the Bell-Evans-Polanyi relationship as they stabilize or destabilize reactants or products.
- Experimentally estimated excited aromatic stabilization energies can be as high as 20 kcal/mol, which would have significant influence on *reactivity*.
- New photochemical *reactions* can be developed and explained based on excited state antiaromaticity.
- Photophysical *properties* such as excitation energies can be tuned by considering the (anti)aromaticity of both the ground and the excited states.

I believe that there are many fruitful lines of future research that could build upon these results, mainly in the direction of developing new photoreactions and new materials. Some of these are:

- What is the influence of aromaticity/antiaromaticity in more complex molecules that contain multiple chromophores?
- Is it more fruitful to develop photoreactions based on gaining aromaticity or alleviating antiaromaticity?
- How does the knowledge obtained for the triplet excited state apply to the singlet excited state where most photoreactions occur?
- How do the aromaticity-property relationships translate into extended materials, such as polymers, when there is a limited number of simultaneous excitons?

7 Svensk sammanfattning

Inverkan av aromaticitet på struktur, reaktivitet och egenskaper för fotoexciterade molekyler

Fotokemi innebär att kemiska föreningar omvandlas under belysning. Många viktiga fotokemiska processer sker i naturen, t ex fotosyntesen, synen och då D-vitamin bildas i kroppen när huden exponeras för solljus (Bild 1). Allt börjar med att en kemisk förening tar upp synligt eller ultraviolett ljus. Energin i ljuset omvandlas till överskottsenergi hos elektronerna som håller ihop molekylen och man säger att molekylen är (foto)exciterad. Om ljusenergin är tillräckligt stor kan den till och med bryta de kemiska bindningar som håller ihop molekylen. Den kan då reagera med andra molekyler i omgivningen och bilda nya kemiska föreningar och detta kallas fotokemi (Bild 1).

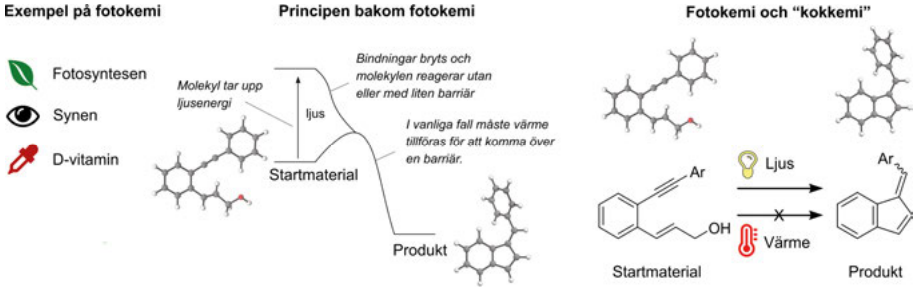

Bild 1. Viktiga exempel på fotokemi, principen för hur fotokemi fungerar och fotokemi jämfört med "kokkemi".

Kemister har under de senaste hundra åren försökt att använda fotokemi för att framställa konstgjorda molekyler i laboratoriet. Anledningen är att det finns vissa fördelar jämfört med den vanliga "kokkemin" där man tillför energi i form av värme istället för ljus (Bild 1). För det första är det mer effektivt att tillföra energi direkt till molekylerna i form av ljus än att värma upp ett stort reaktionskärl med lösningsmedel. Väldesignade fotokemiska processer skulle därför kunna spara mycket energi i den kemiska industrin. För det andra kan man genom fotokemi också få tillgång till kemiska föreningar som idag är mycket svåra att tillverka med konventionella metoder. Potentialen är mycket stor inom tillverkning av t ex läkemedel, jordbrukskemikalier, smakämnen och doftämnen.

Tyvärr har det varit svårt att utveckla nya fotoreaktioner. I den vanliga kokkemin är man däremot mycket bättre på att förutsäga hur olika kemiska

föreningar kommer att reagera med varandra. Denna förståelse bygger bland annat på olika typer av tumregler som utvecklats gradvis under de senaste hundra åren. Man kan därför på ett effektivt sätt utveckla nya reaktionstyper och ta fram syntesvägar till eftertraktade föreningar. Inom fotokemin har man inte alls kommit lika långt i utvecklingen av dessa tumregler, och därför är fotokemin svår att använda för kemister som inte är experter inom området.

I den här avhandlingen har jag på en grundforskningsnivå undersökt just en sådan tumregel för fotokemi. Jag har utgått från ett kemiskt begrepp, aromaticitet, som har varit till stor hjälp när man vill förstå den konventionella kokkemin. I de studier som presenteras i avhandlingen har jag kunnat visa att begreppet också är mycket användbart när man ska förstå fotokemi och fotofysik. Jag har här byggt vidare på teoretiska förutsägelser från 1970-talet och andra gruppers arbete de senaste 20–30 åren.

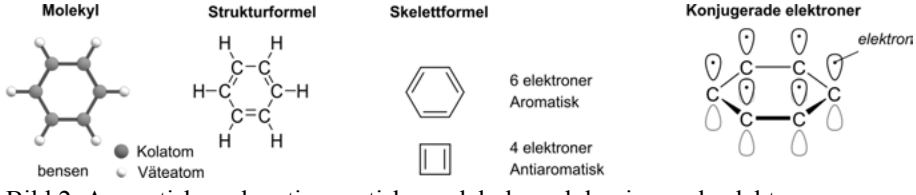

Bild 2. Aromatiska och antiaromatiska molekyler och konjugerade elektroner.

Begreppet aromaticitet används för att beskriva en viss typ av kemiska föreningar där atomerna sitter ihop i en ring (Bild 2). Vissa av elektronerna i ringen är inte bundna till en enskild atom utan delas mellan atomerna – man säger att ringen är konjugerad. Beroende på antalet elektroner i ringen är föreningen aromatisk, *dvs.* extra stabil (2, 6, 10 … elektroner), eller antiaromatisk, *dvs.* extra instabil (4, 8, 12 … elektroner). För de fotoexciterade molekylerna är dessa räkneregler istället omvända. Jag har, i samarbete med mina kollegor och andra forskare, kunnat använda begreppet för att:

- Förklara hur den tredimensionella strukturen hos molekyler förändras när de absorberar ljus. Detta är inte bara viktigt för den grundläggande förståelsen utan skulle också kunna användas för material som ändrar form under belysning.
- Uppskatta hur stor den energimässiga aromatiska stabiliseringen är hos de fotoexciterade molekylerna och hur stabilisering och destabilisering kan kopplas till en ökad eller minskad fotoreaktivitet. Detta är viktig kunskap för att förstå om begreppet är användbart för att utveckla ny fotokemi eller inte.
- Ta fram och förklara nya fotokemiska reaktioner. T ex visade vi att viktiga molekyler som bensen och polyaromatiska kolväten kan addera väte och kisel under belysning. Till och med framtidsmaterialet grafen reagerade.

- Justera vilken våglängd som kemiska föreningar tar upp ljus på och därmed vilken energi de fotoexciterade elektronerna har. Detta kan vara viktig kunskap för framtida forskning på kolbaserad elektronik.

Resultaten som presenteras i avhandlingen visar tydligt att aromaticitetsbegreppet är ett användbart verktyg för att förstå fotokemi och fotofysik. Den nya kunskapen utgör en pusselbit som andra forskare kan bygga vidare på för att försöka utveckla nya och mer effektiva fotokemiska reaktioner och nya material, t ex för tillverkning av läkemedel eller kolbaserad elektronik.

8 Acknowledgements

First, I would like to thank my supervisor, Henrik Ottosson, for accepting me as a PhD student in his group, for very fruitful collaboration during the years and for allowing me substantial freedom to explore chemistry.

Thanks to my second supervisor, Roland Lindh for stimulating discussions about multiconfigurational quantum chemistry and machine learning, and especially for giving me a guided tour of the history of Harvard University.

Thanks to my third supervisor, Burkhard Zeitz for teaching me the little I know about experimental photochemistry and velomobiles.

Thanks to Helena Grennberg, professor for postgraduate studies, for providing very valuable advice during my PhD studies, thesis work and during my first time as a teacher at the university level.

Thanks to past and present members of the Ottosson group. In particular: Rabia Ayub, Aleksandra Denisova and Raffaello Papadakis for your company during almost the entirety of my PhD. A special thanks to Rikard Emanuelsson for teaching me both synthetic organic chemistry and computational chemistry as well as uncountable other things. In no particular order: Christian Dahlstrand, Burkhard O. Jahn, Anup Rana, Sangeeta Yadav, Tomas Slanina, Josene Maria Toldo, Wangchuk Rabten, Ouissam El Bakouri, Julius Tibbelin, Anas Saithalavi, Muhammad Rouf Alvi, Leandro Cid Gomes, Jingjing Wu and Ke An.

My lunch friends at Ångström, Sonja Pullen, Timofey Liseev, Kári Sveinbjörnsson and Kerttu Aitola for friendship over the years.

My adventure buddies Daniel Kovacs, Jia-Fei Poon, Jiajie Yan, Xiao Huang, Cuiyan Li and Rabia Ayub for sharing many experiences and especially the unforgettable trip to the ice hotel in Jukkasjärvi.

For proofreading my thesis: Rabia Ayub, Rikard Emanuelsson, Tomas Slanina and Timofey Liseev.

Groups at Department of Chemistry – Ångström Laboratory

- Roland Lindh and his group, including Ignacio Fernández Galván, Morgane Vacher and Mickaël Delcey, for stimulating journal clubs and seminars. In particular, I would like to thank Ignacio for answering all possible and impossible questions about the (Open)Molcas program.
- Sascha Ott and his group, including Anna Arkhypchuk, Keyhan Esfandiarfard, Brian McCarthy, Ben Johnson, Juri Mai, Timofey Liseev, Nicolas D´Imperio, Ashleigh Castner, Souvik Roy, Asamanjoy Bhunia, Sonja Pullen and Giovanny Parada.
- Anders Thapper and his group, including Michele Bedin, Hemlata Agarwal and Biswanath Das.
- Andreas Orthaber and his group, including Simon Clausing, Arvind K. Gupta, Joshua Green, Muhammad Anwar Shameem and Daniel Morales Salazar.
- Eszter Borbas and her group, including Daniel Kovacs, Ruisheng Xiong, Aritz Perez and Julien Andres.

Groups at BMC

- Adolf Gogoll, Helena Grennberg and their groups, including Sandra Olsson, Anna Lundstedt, Sara Norrehed and Magnus Blom. In particular, Michael Nordlund for introducing me to teaching and beating me badly in tennis and Hao Huang for sharing your knowledge of and passion for the Chinese cuisine. Finally, Xiao Huang for your valuable friendship, countless dinners, activities and badminton matches.
- Lars Engman and his group, including Jiajie Yan, Jia-Fei Poon and Vijay Pal Singh.
- Jan Kihlberg and his group, including Tobias Ankner and Lina Lindfors.
- Lars Baltzer and his group, including Aleksandra Balliu, Jie Yang and Susanna Kärkkäinen.
- Mikael Widersten and his group, including Emil Hamnevik, Thilak Reddy Enugala, Derar El Smadi and Cecilia Blikstad.
- Joseph Samec and his group, including Anon Bunrit, Maxim Galkin, Pemikar Srifa, Alban Cadu and Supaporn Sawadjoon.
- The Renfuel company, including Joakim Löfstedt, Johan Verendel and Alexander Orebom.
- Lukasz Pilarski and his group, including Carina Sollert, Karthik Devaraj and Emilien Demory.
- Peter Dinér and his group, including Laura Mesas-Sánchez and Alba Diaz-Alvarez.
- Lynn Kamerlin and her group, including Alexandre Barrozo, Beat Amrin, Paul Bauer and Fernanda Duarte. Thanks to Lynn for valuable career advice and for kidnapping me at Boston Logan International Airport. Thanks Fernanda for sharing the challenges of being a young scientist and the difficulties of density functional theory.

Collaborators

- Dr. Yoshimitsu Itoh and the Aida group at The University of Tokyo. Thanks to Yoshi and Michihisa Ueda for nice memories at the Gordon Conference on Physical Organic Chemistry in 2015 and for visiting Sweden in dark and cold November.
- Prof. Miquel Solà at University of Girona, Spain and his group. Ferran Feixas and Ouissam El Bakouri for all electronic index calculations.
- Prof. Dongho Kim at Yonsei University, South Korea, and his group. In particular Young Mo Sung and Juwon Oh, who visited Sweden for one month. Thank you for showing me your lab at Yonsei University and around Seoul!
- Prof. Igor Alabugin at Florida State University, USA and his group. It's always great to meet you at various conferences around the world. Thanks to Rana Mohamed for an awesome effort on our common project and Gabriel Dos Passos Gomes for discussing computational chemistry and the challenges of building a scientific career.
- Prof. Patrick Bultinck at Ghent University, Belgium, for a very fruitful collaboration on triplet state homoaromaticity and for cultivating a skeptical scientific mindset.

The Swedish Research Council is acknowledged for funding. The Liljewalchs foundation, Anna Maria Lundin Foundation at Smålands Nation, the Royal Swedish Academy of Sciences, the ÅForsk Foundation and the Knut and Alice Wallenberg Foundation are acknowledged for generous travel grants that allowed me to attend many international conferences.

Thanks to my high school chemistry teacher, Sven Andersson, for igniting my interest in chemistry. Finally, my deepest thanks to my family for continuously encouraging and supporting my thirst for knowledge from childhood until today.

9 References

1 Klán, P.; Wirz, J. *Photochemistry of Organic Compounds: From Concepts to Practice*; Wiley: Chichester, 2009.
2 Gleiter, R.; Haberhauer, G. *Aromaticity and other conjugation effects*; Wiley-VCH: Weinheim, 2012.
3 Baird, N. C. *J. Am. Chem. Soc.* **1972**, *94*, 4941.
4 Aihara, J. *Bull. Chem. Soc. Jpn.* **1978**, *51*, 1788.
5 Woodward, R. B.; Hoffmann, R. *The Conservation of Orbital Symmetry*; Verlag Chemie: Weinheim, 1970.
6 (a) Dewar, M. J. S. *Tetrahedron* **1966**, *22*, *Supplement 8*, 75. (b) Zimmerman, H. E. *J. Am. Chem. Soc.* **1966**, *88*, 1564.
7 Rosenberg, M.; Dahlstrand, C.; Kilså, K.; Ottosson, H. *Chem. Rev.* **2014**, *114*, 5379.
8 Papadakis, R.; Ottosson, H. *Chem. Soc. Rev.* **2015**, *44*, 6472.
9 Stanger, A. *Chem. Commun.* **2009**, 1939.
10 Cyrañski, M. K.; Krygowski, T. M.; Katritzky, A. R.; Schleyer, P. v. R. *J. Org. Chem.* **2002**, *67*, 1333.
11 Gershoni-Poranne, R.; Stanger, A. *Chem. Soc. Rev.* **2015**, *44*, 6597.
12 Feixas, F.; Matito, E.; Poater, J.; Solà, M. *J. Phys. Chem. A* **2007**, *111*, 4513.
13 Yarkony, D. R. *Chem. Rev.* **2012**, *112*, 481.
14 Cramer, C. J. *Essentials of computational chemistry: theories and models*, 2nd ed.; Wiley: Chichester, 2004.
15 Koch, W.; Holthausen, M. C. *A Chemist's Guide to Density Functional Theory*, 2nd ed.; Wiley-VCH: Weinheim, 2001.
16 Adamo, C.; Jacquemin, D. *Chem. Soc. Rev.* **2013**, *42*, 845.
17 González, L.; Escudero, D.; Serrano-Andrés, L. *ChemPhysChem* **2012**, *13*, 28.
18 Raghavachari, K.; Trucks, G. W.; Pople, J. A.; Head-Gordon, M. *Chem. Phys. Lett.* **1989**, *157*, 479.
19 Roos, B. O.; Taylor, P. R.; Siegbahn, P. E. M. *Chem. Phys.* **1980**, *48*, 157.
20 Bachrach, S. M. *Wiley Interdiscip. Rev. Comput. Mol. Sci.* **2014**, *4*, 482.
21 Gonthier, J. F.; Steinmann, S. N.; Wodrich, M. D.; Corminboeuf, C. *Chem. Soc. Rev.* **2012**, *41*, 4671.
22 Cyrański, M. K. *Chem. Rev.* **2005**, *105*, 3773.
23 Krygowski, T. M.; Szatylowicz, H.; Stasyuk, O. A.; Dominikowska, J.; Palusiak, M. *Chem. Rev.* **2014**, *114*, 6383.
24 Feixas, F.; Matito, E.; Poater, J.; Solà, M. *Chem. Soc. Rev.* **2015**, *44*, 6434.
25 (a) Schleyer, P. v. R.; Pühlhofer, F. *Org. Lett.* **2002**, *4*, 2873. (b) Wannere, C. S.; Moran, D.; Allinger, N. L.; Hess, B. A.; Schaad, L. J.; Schleyer, P. v. R. *Org. Lett.* **2003**, *5*, 2983. (c) Zhu, J.; An, K.; Schleyer, P. v. R. *Org. Lett.* **2013**, *15*, 2442. (d) An, K.; Zhu, J. *Eur. J. Org. Chem.* **2014**, *2014*, 2764.
26 Chen, Z.; Wannere, C. S.; Corminboeuf, C.; Puchta, R.; Schleyer, P. v. R. *Chem. Rev.* **2005**, *105*, 3842.

27 Fallah-Bagher-Shaidaei, H.; Wannere, C. S.; Corminboeuf, C.; Puchta, R.; Schleyer, P. v. R. *Org. Lett.* **2006**, *8*, 863.
28 (a) Stanger, A. *J. Org. Chem.* **2006**, *71*, 883. (b) Jiménez-Halla, J. O. C.; Matito, E.; Robles, J.; Solà, M. *J. Organomet. Chem.* **2006**, *691*, 4359.
29 Gershoni-Poranne, R.; Stanger, A. *Chem. - Eur. J.* **2014**, *20*, 5673.
30 Geuenich, D.; Hess, K.; Köhler, F.; Herges, R. *Chem. Rev.* **2005**, *105*, 3758.
31 Matito, E.; Duran, M.; Solà, M. *J. Chem. Phys.* **2005**, *122*, 14109.
32 Noorizadeh, S.; Shakerzadeh, E. *Phys. Chem. Chem. Phys.* **2010**, *12*, 4742.
33 Bultinck, P.; Ponec, R.; Van Damme, S. *J. Phys. Org. Chem.* **2005**, *18*, 706.
34 Oh, J.; Sung, Y. M.; Mori, H.; Park, S.; Jorner, K.; Ottosson, H.; Lim, M.; Osuka, A.; Kim, D. *Chem* **2017**, *3*, 870.
35 Bonačić-Koutecký, V.; Koutecký, J.; Michl, J. *Angew. Chem., Int. Ed.* **1987**, *26*, 170.
36 Casida, M. E.; Huix-Rotllant, M. *Annu. Rev. Phys. Chem.* **2012**, *63*, 287.
37 Williams, R. V. *Chem. Rev.* **2001**, *101*, 1185.
38 Jorner, K.; Jahn, B. O.; Bultinck, P.; Ottosson, H. *Chem. Sci.* **2018**, *9*, 3165.
39 Jorner, K.; Dreos, A.; Emanuelsson, R.; El Bakouri, O.; Fdez. Galván, I.; Börjesson, K.; Feixas, F.; Lindh, R.; Zietz, B.; Moth-Poulsen, K.; Ottosson, H. *J. Mater. Chem. A* **2017**, *5*, 12369.
40 Carey, F. A.; Sundberg, R. J. *Advanced Organic Chemistry. Part A: Structure and Mechanisms*, 5th edition; Springer: New York, 2007.
41 Ueda, M.; Jorner, K.; Sung, Y. M.; Mori, T.; Xiao, Q.; Kim, D.; Ottosson, H.; Aida, T.; Itoh, Y. *Nat. Commun.* **2017**, *8*, 346.
42 Wu, J. I.; Fernández, I.; Mo, Y.; Schleyer, P. v. R. *J. Chem. Theory Comput.* **2012**, *8*, 1280.
43 Nonhebel, D. C. *Chem. Soc. Rev.* **1993**, *22*, 347.
44 Mohamed, R. K.; Mondal, S.; Jorner, K.; Faria Delgado, T.; Lobodin, V. V.; Ottosson, H.; Alabugin, I. V. *J. Am. Chem. Soc.* **2015**, *137*, 15441.
45 Papadakis, R.; Li, H.; Bergman, J.; Lundstedt, A.; Jorner, K.; Ayub, R.; Haldar, S.; Jahn, B. O.; Denisova, A.; Zietz, B.; Lindh, R.; Sanyal, B.; Grennberg, H.; Leifer, K.; Ottosson, H. *Nat. Commun.* **2016**, *7*, 12962.
46 Popov, I. A.; Bozhenko, K. V; Boldyrev, A. I. *Nano Res.* **2012**, *5*, 117.
47 Jorner, K.; Emanuelsson, R.; Dahlstrand, C.; Tong, H.; Denisova, A. V; Ottosson, H. *Chem. - Eur. J.* **2014**, *20*, 9295.
48 Ayub, R.; El Bakouri, O.; Jorner, K.; Solà, M.; Ottosson, H. *J. Org. Chem.* **2017**, *82*, 6327.
49 Jorner, K.; Feixas, F.; Ayub, R.; Lindh, R.; Solà, M.; Ottosson, H. *Chem. - Eur. J.* **2016**, *22*, 2793.
50 (a) Möllerstedt, H.; Piqueras, M. C.; Crespo, R.; Ottosson, H. *J. Am. Chem. Soc.* **2004**, *126*, 13938. (b) Rosenberg, M.; Ottosson, H.; Kilså, K. *Phys. Chem. Chem. Phys.* **2011**, *13*, 12912.
51 Hoffmann, R. *Angew. Chem., Int. Ed.* **1982**, *21*, 711.
52 Emanuelsson, R.; Wallner, A.; Ng, E. A. M.; Smith, J. R.; Nauroozi, D.; Ott, S.; Ottosson, H. *Angew. Chem., Int. Ed.* **2013**, *52*, 983.
53 Yamaguchi, S.; Tamao, K. *J. Chem. Soc. Dalton Trans.* **1998**, 3693.
54 Zeng, Z.; Shi, X.; Chi, C.; López Navarrete, J. T.; Casado, J.; Wu, J. *Chem. Soc. Rev.* **2015**, *44*, 6578.
55 Sanvito, S. *Chem. Soc. Rev.* **2011**, *40*, 3336.
56 Streifel, B. C.; Zafra, J. L.; Espejo, G. L.; Gómez-García, C. J.; Casado, J.; Tovar, J. D. *Angew. Chem., Int. Ed.* **2015**, *54*, 5888.

Acta Universitatis Upsaliensis

Digital Comprehensive Summaries of Uppsala Dissertations from the Faculty of Science and Technology 1679

Editor: The Dean of the Faculty of Science and Technology

A doctoral dissertation from the Faculty of Science and Technology, Uppsala University, is usually a summary of a number of papers. A few copies of the complete dissertation are kept at major Swedish research libraries, while the summary alone is distributed internationally through the series Digital Comprehensive Summaries of Uppsala Dissertations from the Faculty of Science and Technology. (Prior to January, 2005, the series was published under the title "Comprehensive Summaries of Uppsala Dissertations from the Faculty of Science and Technology".)

Distribution: publications.uu.se
urn:nbn:se:uu:diva-349229

ACTA
UNIVERSITATIS
UPSALIENSIS
UPPSALA
2018